The JLab Hypernuclear Collaboration
May 3, 2013

Jefferson Lab PAC 40

Dear PAC:
We are the JLab Hypernuclear Collaboration. We are the combined former Hall's A and C
Hypernuclear collaborations. We represent several Institutions from around the world, including:
INFN, Tohoku University, Hampton University, Florida International University, and Jefferson
Lab. In the past our combined collaborations have successfully started a program of
Hypernuclear Spectroscopy using separate equipment setups in Hall A and Hall C respectively.
We have, using the $(e,e'K^+)$ reaction, explored the spectroscopy of various Hypernuclei
including $^7_\Lambda$He, $^9_\Lambda$Li, $^{10}_\Lambda$Be, $^{12}_\Lambda$B, $^{16}_\Lambda$N, $^{28}_\Lambda$Al, $^{52}_\Lambda$V with sub MeV resolution in both Halls as well
as working to improve our understanding of the elementary electromagnetic kaon production
process.

With the advent of the 12 GeV era at JLab we felt it was in our best interest and the best interest
of furthering the field of Strangeness in Nuclear Physics to combine our experiences and
expertise to pursue the next generation of Hypernuclear Physics Experiments at JLab. To that
end we have developed a scheme that takes the best of both Hall's and combines them to make
one overall improved setup. We get improved count rates from Hall C and improved signal over
background, ease of calibration, and greater kinematic flexibility at some cost in count rate from
Hall A.

With the development of this new scheme we have assembled a program of sub-experiments that
takes advantage of its strong points and does much to further the world's understanding of
Strangeness in Nuclei. The five sub-experiments address:

- Elementary kaon electroproduction
- Spectroscopy of light Λ-Hypernuclei
- Spectroscopy of medium to heavy Λ-Hypernuclei
- Pion decay spectroscopy

They provide invaluable information on:
- ΛN interaction
- Charge Symmetry Breaking (CSB) in the Λ-N interaction
- Limits of the mean field description of nuclei and hypernuclei
- Λ binding energy as a function of A for different nuclei than those probed with
  hadrons
- Structure of tri-axially deformed nucleus using Λ as a probe.

- Energy level modification effects by adding a Λ

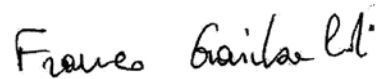- The role of the 3 body ΛNN interaction in Hypernuclei and Neutron Stars

We present to you a proposal that includes all of those sub-experiments.
The following general abstract does much to explain the overall Physics impact such a program
would have. We submit the sub-experiments to you in the proposal document and hope you will

consider their combined affect in your deliberations.

While solidification of our plans and preparation of the proposal has precluded our formal pursuit of their status as "Hall A Collaboration" experiments, we fully intend to pursue this in the future.
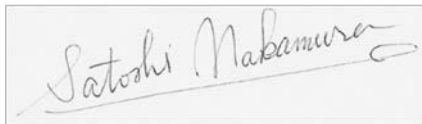
Sincerely,

Franco Garibaldi, Professor, INFN Rome and Istituto Superiore di Sanita

John J. LeRose, Staff Scientist, Thomas Jefferson National Accelerator Facility

Pete Markowitz, Professor of Physics, Florida International University

Satoshi N. Nakamura, Associate Professor of Physics, Tohoku University

Joerg Reinhold, Associate Professor of Physics, Florida International University

Liguang Tang, Professor of Physics, Hampton University

Proposal to PAC 40 for

A Study with High Precision on
the Electro-production of the Λ and Λ-Hypernuclei
in the Full Mass Range

P. Bydžovský[1], F. Cusanno[2], Y. Fujii[3], F. Garibaldi[4], J.J. LeRose[5], P. Markowitz[6], D.J. Millener[7,]
S.N. Nakamura[7], J. Reinhold[6], L. Tang[5,8],G. M. Urciuoli[4], …………………………………………….
On behalf of JLab Hypernuclear Collaboration

[1] *Nuclear Physics Institute, Řež near Prague, Czech Republic*
[2] *Physik Department, Technische Universitaet Muenchen, D-85748 Garching b. Muenchen, Germany*
[3] *Department of Physics, Tohoku University, Sendai, 980-8578, Japan*

[4] *Istituto Nazionale di Fisica Nucleare, Sezione di Roma, Gr. Coll. Sanita',Viale Regina Elena 299, Rome, Italy*
[5] *Thomas Jefferson National Accelerator Facility, Newport News, Virginia 23606, USA*
[6] *Florida International University, Miami, Florida 33199, USA*
[7] *Brookhaven National Laboratory, Upton, New York 11973, USA*
[8] *Department of Physics, Hampton University, Hampton, Virginia, 23668, USA*

Abstract

The JLab hypernuclear collaboration which was newly formed by merging Hall-A hypernuclear collaboration and Hall-C HKS-HES collaboration, is going to propose a comprehensive hypernuclear program at JLab after the CEBAF 12 GeV upgrade. This proposal contains four parts: 1) General introduction of the entire program and common experimental setups, 2) the study of hypernuclei with the $(e,e'K^+)$ reaction spectroscopy, 3) the decay pion spectroscopy of electro-produced hypernuclei and 4) summary.

An ambitious and challenging experimental program started at Jefferson Lab 10 years ago, high-resolution hypernuclear spectroscopy via the $(e,e'K^+)$ reaction. Data have been taken in both Hall A and Hall C on p-shell and medium-mass targets, providing clean spectra with sub-MeV energy resolution. The analysis is finished for some targets (^{7}Li, ^{9}Be, ^{12}C, ^{16}O), or in an advanced state for others (^{10}B, ^{28}Si, ^{52}Cr). The results confirm the power of the technique and its important role in hypernuclear physics. It has advantages in energy resolution over hadronic probes and complements them in being a dominantly spin-flip reaction as opposed to a non-spin flip reaction. The greater strength observed for the low-lying excited states of $^{12}_\Lambda$B relative to the ground state is an example of the advantage sometimes afforded by the spin-flip capability. Gamma-ray spectroscopy, while extremely powerful, is limited to particle-bound states (and thus in light nuclei to Λ's in s orbits). The $(e,e'K^+)$ reaction enables the determination of binding energies with high precision because of the calibration provided by the elementary reaction on hydrogen. The elementary interaction itself, fundamental to the interpretation of hypernuclear data, can be studied at forward angles where there is a lack data and a wide disagreement among existing models. This proposal deals with a new series of experiments on several targets both for mass spectroscopy and pion decay spectroscopy. This will make significant contributions to hypernuclear physics research for the next decade(s) in the framework of the research either ongoingor planned in this field in the world. For this reason, since it is essential for further theoretical study of hypernuclei to collect enough information about Λ production on nucleons and about excitation spectra of a wide variety of Λ-hypernuclei, a continuation of the successful hypernuclear program at JLab is proposed. The new experimental design not only widens and deepens the physics range but also dramatically improves production yield and efficiency.

Even though plans for various new hypernuclear physics studies exist at different facilities, the precision, accurate mass spectroscopy from the JLab program has an unchallengeable position, in addition to the clearly known common advantages of electro-production (such as the size of momentum transfer, extra spin transfer from the virtual photon, converting a proton to a Λ for neutron rich hypernuclei etc.). Using the pion decay spectroscopy technique will complement the mass spectroscopy part of the proposal. Namely this proposal addresses novel systematic studies of light hypernuclei using pionic weak 2-body decay. It aims to determine structural properties, such as binding energies, lifetimes, production mechanism, charge symmetry breaking (CSB) effects in mirror pairs, and in-medium effects on electric and magnetic properties of hypernuclei.

The 6 GeV experiments provided sufficient experience to establish the new program for CEBAF in the 12 GeV era. The outcome of the present activity is the base for building this experimental program, in the framework of the hypernuclear research that will take place in other laboratories with different, complementary techniques.

The new program represents an optimization that can broaden the physics investigation range and topics and can also greatly improve production efficiency, maximizing the physics output dramatically.

Part 1. General Introduction

1. Hypernuclear Physics

The physics of hypernuclei, multibaryonic systems with non-zero strangeness, is an important branch of contemporary nuclear physics at low energy (structure, energy spectra and weak decays of hypernuclei) as well as at intermediate energy (production mechanism). The Λ hypernucleus is a long-lived baryonic system ($\tau=10^{-10}$s) and provides us with a variety of nuclear phenomena. The hyperon is not affected by the Pauli principle and can penetrate deeply inside the nucleus permitting measurements of the system's response to the stress imposed on it. The study of its propagation can reveal configurations or states not seen in other ways. The study also gives important insight into the structure of ordinary nuclear matter.

New nuclear structures or unknown properties of the baryonic interaction, which cannot be seen from the investigation of ordinary nuclei with conventional probes, may manifest themselves in hypernuclei, providing indispensable information on the flavor SU(3) basis for baryonic systems. To create a unified description of the baryonic interaction within the flavor SU(3) basis, one must understand baryonic interactions beyond nucleon-nucleon (NN) interactions, such as hyperon-nucleon (YN) and hyperon-hyperon (YY) interactions. Spectroscopic investigation of Λ hypernuclei, a nuclear many-body system containing one Λ particle, provides a unique and currently the only practical tool to study the ΛN interaction, since direct ΛN scattering experiments are technically difficult. Since the Λ decays only weakly and has a relatively long lifetime, Λ hypernuclei feature narrow states commonly described by coupling of low-lying core states to a Λ in low level shell states (s, p, ...) with widths ranging from a few to ~ 100 keV depending on the decay channels (weak decay, EM transitions, and nucleon emissions or breakups at high excitation levels). This makes spectroscopic studies possible.

One novel feature of the ΛN interaction is due to the fact that the Λ has isospin 0. This prevents one-pion-exchange (OPE) due to isospin conservation in the strong interaction. This means that the OPE that gives rise to the long-range component in the NN interaction is missing in the ΛN interaction. However, OPE can couple the ΛN and ΣN channels in the strangeness -1 baryon-baryon interaction and this coupling has to be treated explicitly. This coupling can also give rise to a ΛNN interaction when a Λ is excited to a Σ on one nucleon and de-excited on another nucleon.

A series of free YN and YY one-boson-exchange models have been constructed by the Nijmegen [Rij99] and Julich [Hai05] groups as extensions of NN models that incorporate flavor SU(3) and SU(6) symmetry, respectively. More recently extended-soft-core models that include two-meson exchange [Rij06] and models at next-to-leading order in chiral effective field theory [Hai13]have been developed. Given the paucity of YN scattering data, some known properties of hypernuclei are used to constrain the models.

Few-body systems can be calculated via techniques that can handle the free YN interaction, including the $\Lambda-\Sigma$ coupling. In fact, $\Lambda-\Sigma$ coupling is essential to obtain a consistent description of the s-shell hypernuclei ($^3_\Lambda$H, $^4_\Lambda$H, $^4_\Lambda$He and $^5_\Lambda$He), $\Lambda-\Sigma$ coupling contributes especially strongly to the binding energy of the 0^+ ground states of the A = 4 hypernuclei and also therefore to the ~ 1.1 MeV separation between the 1^+ and 0^+ states of these hypernuclei. The singlet component of the Λ N interaction has to be stronger than the triplet to bind the hypertriton and to contribute positively to the $1^+/0^+$ energy separation.

To be used in shell-model calculations for heavier hypernuclei, an effective interaction has to be constructed via a G-matrix calculation to handle the strong short-range repulsion in the free interactions. The G-matrix elements are usually fitted to obtain an interaction in which the various central, tensor, and spin-orbit components are represented by a number of Gaussian, Yukawa, or OBE radial forms.

Shell-model calculations for hypernuclei start with the Hamiltonian (Y can be a Λ or a Σ)

$$H = H_N + H_Y + V_{NY} \qquad (1)$$

where H_N is some empirical Hamiltonian for the nuclear core, the single-particle H_Y supplies the ~ 80MeV mass difference between Λ and Σ, and V_{NY} is the YN interaction. The shell model basis states are chosen to be of the form

$$\left| \alpha_c \, J_c \, T_c \,, j_Y t_Y \right) J\, T \Big\rangle, \qquad (2)$$

where the hyperon is coupled in angular momentum and isospin to eigenstates of the Hamiltonian for the core. This is known as a weak-coupling basis and, indeed, the mixing of basis states in the hypernuclear eigenstates is generally very small. In this basis, the core energies are taken from experiment where possible and from the calculation for the core nucleus otherwise.

For the nuclear p-shell, the ΛN effective interaction can be written [Mil12]:

$$V_{\Lambda N}(r) = V_0(r) + V_\sigma(r)\vec{s}_N \cdot \vec{s}_\Lambda + V_\Lambda(r)\, \vec{l}_{N\Lambda} \cdot \vec{s}_\Lambda + V_N(r)\, \vec{l}_{N\Lambda} \cdot \vec{s}_N + V_T(r)S_{12}, \qquad (3)$$

where $S_{12} = 3(\vec{\sigma}_N \cdot \vec{r})\left(\vec{\sigma}_\Lambda \cdot \vec{r}\right) - \vec{\sigma}_N \cdot \vec{\sigma}_\Lambda$. The five $p_N s_{\Lambda-}$ two-body matrix elements depend on the radial integrals associated with each component in Eq. (3), conventionally denoted by the parameters $\bar{V}, \Delta, S_\Lambda, S_N$ and T. By convention, S_Λ and S_N are actually the coefficients of $\vec{l}_{N\Lambda} \cdot \vec{s}_\Lambda$ and $\vec{l}_{N\Lambda} \cdot \vec{s}_N$. This parameterization applies to the direct ΛN interaction, the ΛN– ΣN coupling interaction, and the direct ΛN interaction for both isospin 1/2 and 3/2.

The direct comparison of structure calculations with hypernuclear binding energies and excitation spectra (often from precise γ-ray measurements) has provided a way of testing and improving YN interaction models.

The comprehension of Baryon-Baryon (BB) interactions is fundamental in order to understand our world and its evolution. However, our current knowledge is limited at the level of strangeness zero particles (p and n). Hence, studying BB interactions (YN and YY) is very important in order to extend our knowledge and seek a unified description of them. Due to the short lifetime of the Y, a direct study of YN interactions is almost impossible but we have a laboratory to study this, the atomic nucleus. As pointed out previously an effective ΛN interaction can be determined from the hypernuclear spectra obtained from various reactions and be used to discriminate between the different hyperon-nucleon (YN) and hyperon-hyperon potentials employed to carry out *ab initio* many-body calculations. The YN interaction, as well as the three-body YNN interaction, have been recently investigated in a number of nuclei, spanning a broad range of mass number, using the Auxiliary Field Diffusion Monte Carlo

(AFDMC) approach [Lon13]. Systematic studies of hyperon interactions in hadronic many body systems may provide a wealth of valuable new information.

The detailed knowledge of the ΛN interaction is important for the following reasons:

      - It provides a check of various generalized models of the baryon-baryon interaction (including hyperons) based on meson-exchange (Nijmegen, Julich, ... potentials) and on quark motivated attempts to describe the short-range part of this interaction. Microscopic calculations in the whole range of A would give a consistent generalized frame to this picture.

      - By comparing the energy spectra of "mirror" hypernuclei, such as $^{12}_{\Lambda}$C, $^{12}_{\Lambda}$B, $^{16}_{\Lambda}$O, $^{16}_{\Lambda}$N one can, in principle, extract some additional information about charge symmetry breaking in the YN interaction, seen many years ago for $^{4}_{\Lambda}$H, $^{4}_{\Lambda}$He and investigated recently in detailed four-body calculations

      - More precise knowledge of the YN and YY interactions can shed some light on the role of strange quarks in the dynamics of the low and intermediate energy baryonic systems.

      - The knowledge of the YN and YY interactions is a prerequisite for the investigation of new forms of hadronic matter. Hyperons are believed to appear in the interior of neutron stars at around 2-3 times nuclear saturation density. Quantitative information on YN, YNN and YY interactions is indispensable to understand the high-density phases of neutron star matter, the occurrence of which may dramatically affect both the equilibrium and non-equilibrium properties of the star. Most theoretical models predict that the appearance of hyperons brings the maximum mass of a stable neutron star down to values incompatible with the recent observation of a star of about two solar masses. While there are indications that this problem may be overcome including the effect of YNN interactions, it may also signal the presence of a non-hadronic phase, *i.e.* of deconfined quark matter, in the inner core of the star.

      The elementary interaction is fundamental to the interpretation of hypernuclear data. It has to be studied at forward angles where there is a lack of data and a wide disagreement among existing models. Measurements performed at small values of the virtual-photon mass are important to the understanding of the process with virtual photons, in the framework of an effective Lagrangian this means a better knowledge of the couplings of the virtual photon with baryon fields (the longitudinal couplings).

      While the spin-independent central parts of the YN and YY interactions are to some extent known, information on the non-central and spin-dependent pieces is scarce or missing. High precision data on light hypernuclei (A=3, 4) are of vital importance for the accurate determination of the unknown parts of the YN and YY interactions.

From the theoretical point of view, these systems can be treated using *ab initio* methods. Within these approaches the interactions are described by *bare* potentials, accounting for both two- and three-baryon forces, and the Schroedinger equation is solved using the variational and Green Function Monte Carlo techniques.

The structure of medium (A = 16) and heavy (A = 90) nuclei is mainly dictated by mean-field dynamics. As a consequence, to a large extent these systems can be understood in terms of quasi particle states associated with the energy spectrum of a static nuclear potential, which is determined self-consistently by the baryons themselves. While for nucleons this picture strictly applies to states close the respective Fermi level, recent measurements of the spectral functions of several single Λ hypernuclei carried out at KEK provide most impressive evidence that in these systems the dominance of single-particle motion persists over the full spectral range, from the deepest bound s-orbit up to the valence orbits of higher angular momentum. Up to now, these data are the best proof ever of quasi particle motion in a strongly interacting system**.**

However, the existing data do not resolve the spectral fine structure, introducing uncertainties into the theoretical analyses. This inhibits a precise determination of the various contributions to the spectral distributions.

The wealth of available (e,e'p) data, while unambiguously confirming the validity of the nuclear shell model, have shown its limitations and the importance of correlation effects, leading to a sizable depletion of the quasi particle states. The results obtained from different many-body microscopic many-body approaches, such as G-matrix perturbation theory, Correlated Basis Function (CBF) perturbation theory and Monte Carlo techniques, have provided convincing evidence that the inclusion of the correlation structure induced by the bare nuclear potentials is needed to explain the data at a fully quantitative level. The extension of these approaches to study hypernuclei does not involve conceptual difficulties. For example, the AFDMC approach has been recently applied to study Λ-hypernuclei with mass number up to 91, and can be readily extended to heavier systems, such as ^{208}Pb. Combining the results of the AFDMC studies and the existing models of the ^{208}Pb spectral function, the formalism successfully employed to describe the (e,e'p) cross section can be readily generalized to the case of Λ electroproduction.

Indeed, the relevance of the mean field approximation in nuclear physics is one of the questions related to the role that the substructure of nucleons plays in the nucleus. To this respect, information about the "distinguishability" of a Λ hyperon as baryon in the nuclear medium can be obtained in principle by systematic spectroscopic analyses, studying the mass number dependence of the binding energies that could differ depending on whether a hyperon keeps its identity as a baryon in a nucleus or not. In other words, the quark picture and the baryon picture of Λ hypernuclear states would yield different hypernuclear mass dependences of the Λ binding energies [Dov87]. This seems to be ruled out by the analysis of experiments with hadron probes [Has06, Hase96]. That show that the single-particle nature of a Λ hyperon persists to first order even for the deeply bound orbits of Λ hypernuclei as heavy as ^{208}Pb. Nevertheless, very precise measurements of binding energies in heavy Λ hypernuclei may provide clues for further discussion about the nature of a baryon in a nucleus. On the other hand, the results of (e,e'p) experiments on ^{208}Pb, designed to the observe the quenching of the spectroscopic factors [Qui88, Bat01] for deeply bound proton orbits, show that the mean field description fails to describe nuclei in the ^{208}Pb region. So spectroscopic investigation of heavy Λ hypernuclei has unique importance .

Until now a large body of data came from two types of highly complementary hypernuclear spectroscopy techniques: reaction based spectroscopy *(with hadron probes)* and gamma spectroscopy. Reaction spectroscopy, which directly populates hypernuclear states, reveals the level structure in the Λ bound region and can even study excited states between the nucleon emission threshold and the Λ emission threshold. It provides information on the Lambda hypernuclear structure and the Λ emission threshold. The information on the Lambda hypernuclear structure and ΛN interaction is obtained through the determination of the hypernuclear masses, reaction cross section, angular distributions etc… The gamma ray spectroscopy achieves ultra-high resolution (typically a few keV). It is a powerful tool for investigation of the spin dependent part of the ΛN interaction, which requires precise information on the level structure of hypernuclei. Both these powerful techniques have limitations, first limited energy resolution and small spin-flip amplitudes, and second the access only to hypernuclear states below nucleon emission threshold. In fact, the hypernuclear gamma-ray measurements give extremely high-precision energy level intervals, while the precision of the energy levels given by the (e, e'K$^+$) reaction spectroscopy can be in the range of 20-30 keV,

which is about one order of magnitude worse than gamma-ray measurement. However, the advantage of being able to simultaneously observe more complete structures, as well as to provide precise absolute binding energy is obvious. For transitions with energy larger than 1 MeV, a Ge detector's efficiency decreases quickly, and thus statistics becomes a major problem for the current gamma spectroscopy program using the Ge detector technique.

Even though plans for various new hypernuclear physics studies exist at other facilities exist, the precision, accurate mass spectroscopy from the JLab program has an unchallengeable position, in addition to the clearly known common advantages of electro-production (such as the size of momentum transfer, extra spin transfer from virtual photon, converting proton to Λ for neutron rich hypernuclei and *etc.*).

The role and the importance of the high pecision hypernuclear reaction spectroscopy program at Jefferson Lab is clear. The very good energy resolution makes it possible to :

- identify unambiguously the centroids of the various components of the spectral functions
- extract information on the spin-orbit splitting as a function of the mass of the core nucleus
- distinguish in the spectral patterns between effects from the static spin-orbit potential and dynamical self-energies due to core polarization, e.g. by observations of rays from core transitions
- use the derived spectral information to determine the corresponding interaction parameters self consistently (either in a non-relativistic Hartree-Fock or a relativistic mean field calculations)
- determine by a theoretical analysis the genuine density dependence of YN interactions which could be achieved either by observing an orbital with given spin and parity over a range of nuclear core masses or by scanning the spectral functions of various angular momenta and multipolarities in a given hypernucleus, keeping the mass number fixed.

The results of the experiments performed in Hall A and Hall C showed the power of this technique in partially overcoming the mentioned limitations on gamma decay spectroscopy and hadron probe reaction techniques, and being fully complementary: i.e having much better energy resolution with respect to the hadron probe reactions, and accessing spin flip amplitude excitations. This is shown by the recent results on ^{7}Li, ^{9}Be, ^{12}C, ^{16}O, ^{28}Si. Much better energy resolution and new strength in the core excited part of the spectrum was obtained.

New experiments allowing one to study with high energy resolution the single particle behavior of a lambda hyperon in light nuclei, medium-mass and high mass hypernuclear systems are needed to explore the entire A range (from few body to ^{208}Pb). This will allow precision measurement of the single particle levels addressing the degree of non-locality of the effective Λ-N potential.

Moreover, the pion decay spectroscopy (an essential complement to the mass spectroscopy part of the proposal) addresses novel systematic studies of light hypernuclei using the pionic weak 2-body decay. It aims to determine structural properties, such as binding energies, lifetimes, production mechanism, charge symmetry breaking (CSB) effects in mirror pairs, and in-medium effects on electric and magnetic properties of hypernuclei. The highlights of the proposed program include:

1. High precision measurements of binding energies of hypernuclear ground and isomeric states;

2. Studies of exotic, extremely rich halo hypernuclei such as superheavy hydrogen ^{6}H;

3. Measurements of electromagnetic rates (and moments);

4. Studies of the production of neutron-rich hypernuclei by means of multi-fragmentation; and

5. CSB studies in mirror pairs.

In conclusion, the proposed experiments will provide key information, not obtainable with the same precision by any other experiment at any other facility, in the study of hypernuclei and Λ-N interaction.

References

[Rij99] Th.A. Rijken, V.J.G. Stoks, Y. Yamamoto, *Phys. Rev.* **C 59**, 21 (1999).

[Hai05] J. Haidenbauer and Ulf-G. Meissner, *Phys. Rev.* **C 72**, 044005 (2005).

[Rij06] Th.A. Rijken, Y. Yamamoto, *Phys. Rev.* **C 73**, 044008 (2006).

[Hai03] J. Haidenbauer *et al.*, arXiv:1304.5339

[Mil12] D.J. Millener, *Nucl. Phys.* **A 881**, 298 (2012).

[Lon13] D.Lonardoni, S.Gandolfi,and F.Pederiva, ArXiv:1301.7472v2 (2013).

[Dov87] C.B. Dover, *Proc. Int. Sympo. on Medium Energy Physics*, Beijing. World Scientifics, Singapore, 1987, p. 257

[Has06] O. Hashimoto and H. Tamura, *Progress in Particle and Nuclear Physics* **57** (2006).

[Hase96] T. Hasegawa *et al, Phys. Rev.* **C53** (1996) 1210

[Qui88] E. Quint, Ph.D. "Limitationd of the Mean – Field Description for nueli in the Pb-region, obeserved with the (e,e'p) Reaction". Thesis Universiteit van Amsterdam 1988.

[Bat01] M.F.Van Batenburg, *"Deeply bound protons in ^{208}Pb"*, Thesis Universiteit van Amsterdam (2001).

2. Experimental Methods and the Expected Yield of Hypernuclei

2.1 Selection of the experimental hall and spectrometers to be used

The LOI [Appendix I] presented two possible options for future hypernuclear physics experiments: (1) Septum+HRS/Septum+HKS in Hall A, capable of using 2-pass beam with energy of 4.5238GeV (high energy option) and (2) Septum+HES/Septum+HKS in Hall C, using 1-pass beam with energy of 2.3238 GeV (low energy option). After careful consideration of the merits of the physics, the experimental conditions, and the quality of the expected results, the collaboration has chosen the high energy option in Hall A.

Detailed reasons of the decision can be found in the Appendix II. Let us summarize them briefly:

1. The high beam energy option provides lower e' rates, since Bremsstrulung (roughly proportional to Z^2 in the target) is highly suppressed and results in a better signal-to-accidental background ratio. This is essential for the heavy target.

2. This option Avoids the Splitter which optically couples the e' and K spectrometers, analysis and calibration can be much simpler at some cost in yield.

3. In order to use higher beam energy (4.5 GeV) with the same virtual photon energy as Hall-C (E_γ~1.5 GeV) where the Λ production cross section is maximum, the e' momentum should be about 3 GeV/c and thus HRS in Hall-A is necessary. Large kaon decay loss due to a long path length can be overcome by using the HKS as the K spectrometer instead of HRS. Decoupling of two spectrometers systems will make analysis and calibration simpler.

4. Although the energy resolution for the high beam energy option will be slightly worse than the low beam energy option, it can still reach about the 600-800 keV (FWHM), which is still good enough to have a precision study of the hypernuclear spectroscopy.

The new setup adopts the advantages of both previous Hall-A and Hall-C setups.

In addition to Septa+HKS+HRS magnets, two additional spectrometers (HES and ENGE split-pole) will be placed at backward angles to study decay π^- spectroscopy. Therefore, two independent experiments can share the same beam time and have more physics output.

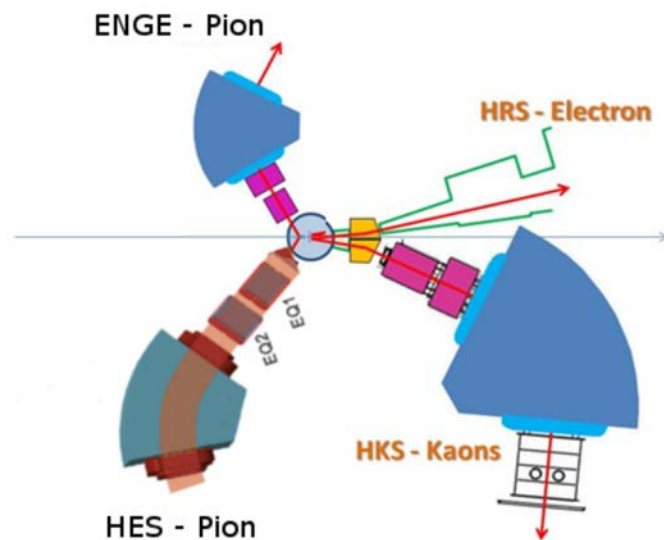Figure 2.1 shows a schematic illustration of the proposing experiment.

Figure 2-1: Schematic illustration of the proposing experiment. For reaction spectroscopy, HKS for K+, HRS for e' are used with septum magnets. HES and ENGE split-pole are placed as pion spectrometers for decay pion spectroscopy.

Design plans of the septum magnets are given in Appendix II. The HKS Septum magnet needs to be newly fabricated while the previously used super-conducting septum could be used for the HRS side.

All four spectrometers are well known and have been previously used. HKS, HES and Enge were used with the splitter magnet rather than a septum magnet, but a septum magnet is optically very similar to the splitter. Septum magnets were successfully used with HRS and the design concept is well established. Parameters of the spectrometers are summarized in Table 2-I.

Kaon identification in HKS and electron selection in HRS are well established. Detailed information about HKS, HES, ENGE detectors in spectrometers are given in E01-011, E05-115 Proposal and Technical Review documents.

Here is a brief explanation of the kaon identification power of the HKS detector package. The HKS detectors will be used for the proposed experiments. Two sets of drift chambers for tracking, three layers of plastic scintillator arrays for trigger and time-of-flight measurement, three layers of aerogel Cherenkov counters (Panasonic, n=1.05) and two layers of water Cherenkov counters for pion and proton suppression. In the on-line trigger, rejection by Cherenkov counters were relatively loose so as not to lose kaons at the trigger level. Therefore, π^+ and proton rejection efficiencies were set at 1% and 4.5% levels respectively in the E05-115. In the off-line analysis, tighter cuts by Cherenkov counters and time-of-flight information gave 10^{-6} and 10^{-5} rejection power. In E05-115, $\pi^+ : K^+ :p$ ratio in the K+ spectrometer was originally 10000:1:2000, 90:1:90 in the on-line trigger and 0.01:1:0.02 after the off-line analysis. Very clean kaon identification was realized.

Table 2-I: Parameters of the spectrometers

Beam condition
Beam energy   4.52 GeV
Beam momentum stability 3×10^{-5} (rms)

General configuration   Septum + HKS (K^+) + HRS (e') + HES (π^-) + ENGE (π^-)

HKS spectrometer (K^+)
Configuration   Q-Q-D and horizontal 70° bend
Central momentum   1.2 GeV/c
Dispersion   4.7 cm/%
Momentum acceptance   ± 12.5% (1.05-1.35 GeV/c)
Momentum resolution ($\Delta p/p$) 2×10^{-4}
Solid angle   7.5 msr with the septum
                                     (30 msr without septum)
Kaon detection angle   Horizontal : 16° (±4.5°)
Flight path length   9.5 m
Maximum magnetic field   1.6 T (normal conducting magnet)

HRS spectrometer (e')
Configuration   Q-Q-D-Q and vertical 45° bend
Central momentum   3.0 GeV/c
Momentum acceptance   ± 4.5% (2.865-3.135 GeV/c)
Momentum resolution ($\Delta p/p$) 1×10^{-4}
Solid angle   3.5 msr with the septum
e' detection angle   Vertical : 7 ° (±2.5°)
Flight path length   23.4 m

HES spectrometer (π^-)
Configuration   Q-Q-D and horizontal 50° bend
Central momentum   0 - 1.0 GeV/c
Dispersion   3.3 cm/%
Momentum acceptance   ± 17.5 %
Momentum resolution ($\delta p/p$) 2×10^{-4}
Solid angle   7 msr
Maximum magnetic field   1.6 T (normal conducting magnet)

ENGE spectrometer (π^-)
Configuration   Split-pole 40+74° bend
Central momentum   0.12 GeV/c
Dispersion   2.0 cm/%
Momentum acceptance   ± 30.0 %
Momentum resolution ($\delta p/p$) 4×10^{-4}
Solid angle   3.4 msr

2.2 Kinemtics and yield estimation

The definition of the kinematics angles and their limits are illustrated in Fig. 2-2 and the assumed kinematics parameters are listed in Table 2-II.
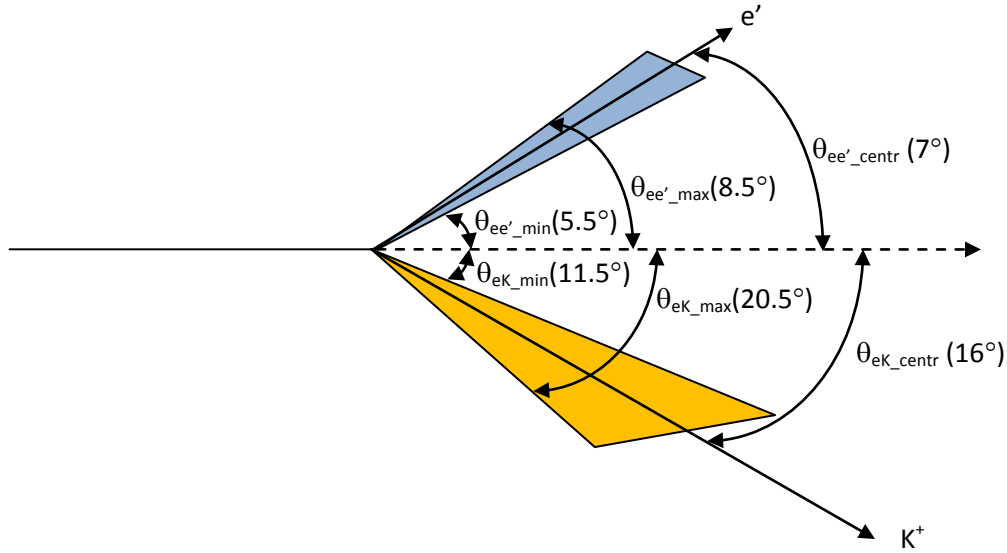

Figure 2-2: Coordination of the kinematics angles of e' and K+ and their limits defined by HRS and HKS.

A GEANT simulation taking into account the realistic and known conditions of HKS and a Transport+Turtle calculation of HRS were performed. No acceptance limitation was included for the new Septum magnet which does not yet have a detailed engineering design. Fig. 2-3 (a) shows the distribution of the Lab virtual photon angle θ_γ with the kinematics shown in Table II and the Septum+HRS acceptances. Most of the virtual photons go into the HKS angular acceptance, i.e. production at $\theta_{\gamma K} = 0°$ is included for most of the photon angular range while the angular range of $\theta_{\gamma K}$ remains large. This ensures high production yield while the angular dependence can be measured without changing the spectrometer configuration. Also, for the elementary production studies, events from interesting Q^2 and $\theta_{\gamma K}$ angle ranges can be specifically selected (see details in the experimental proposal). Fig. 2-3 (b) shows the Q^2 range within the acceptance of the system.

Fig. 2-4 is an illustration of the e' and K^+ momentum correlation for various masses of hyperons (Λ and $\Sigma°$) and ground state hypernuclei ($^{12}_\Lambda$B and $^{208}_\Lambda$Tl). The broadening of the Λ and $\Sigma°$ is from the range of recoil angles. Free Λ and $\Sigma°$ production is important to calibrate the absolute energy scale of the missing mass.

Table 2-II: Basic kinematics parameters of the Septum+HRS and Septum+HKS system.

| Beam energy (12 GeV mode, 2-passes, injector energy included)	4.5238 GeV
E' (HRS) central angle (horizontal and vertical bites)	7° (±1.5° and ±2.5°)
E' (HRS) central momentum (percentage bite)	3.0296 GeV/c (±4.5%)
Virtual photon central angle ($\phi=\pi$)	13.68°
Virtual photon energy range	1.35 – 1.62 GeV
Virtual photon momentum range	1.40 – 1.70 GeV/c
Average Q^2	0.218 $(GeV/c)^2$
K^+ (HKS) central angle (horizontal and vertical bites)	16° (±4.5° and ±2.5°)
K^+ (HKS) central momentum (percentage bite)	1.2 GeV/c (±12.5%)
Lab $\theta_{\gamma K}$ coverage range	0° - 9°
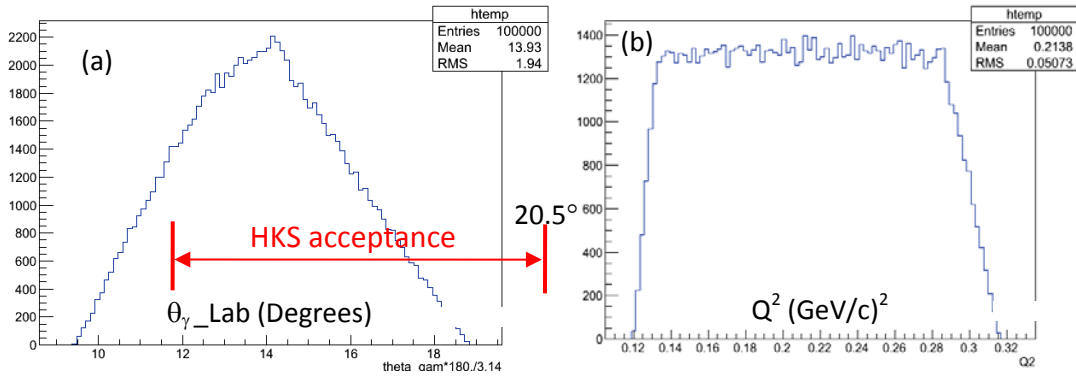
Figure 2-3: (a) Virtual photon angular distribution (symmetric with respect to $\phi = \pi$ plane defined by the central e and e' plane) in Lab system with respect to beam; (b) Q^2 accpetance.
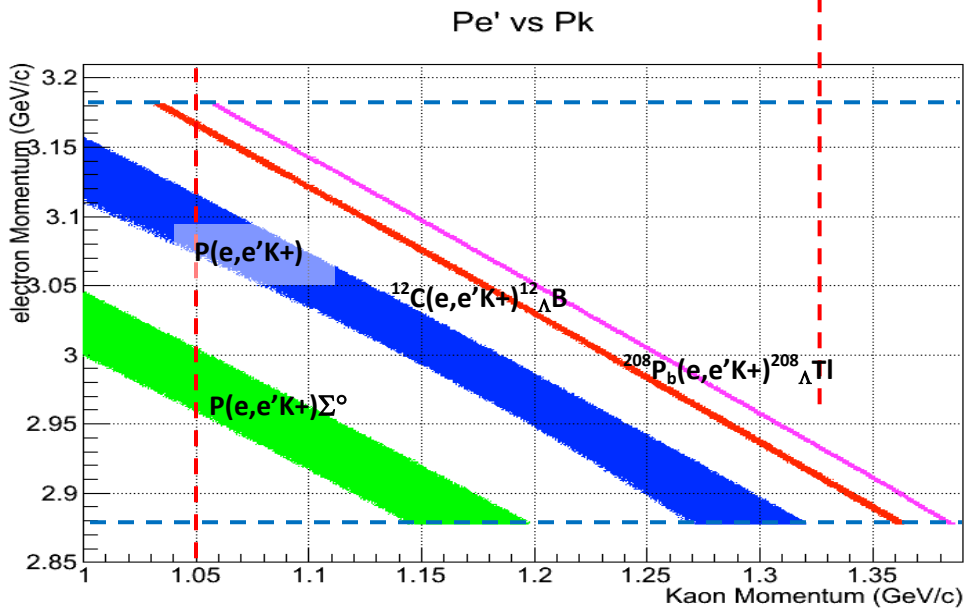

Figure 2-4: Kaon and scattered electrom momenta correlation for various missing masses.

Using the given kinematic parameters, the expected hypernuclear yield was estimated for the new configuration of Septum+HRS/Septum+HKS.

A ^{12}C target is commonly used as a reference in both Hall-A and Hall-C experiments. The photo-production cross section of the ground state of the $^{12}_\Lambda$B hypernucleus ($J^p = 1^-$, 2^-) for E_γ ~1.5 GeV, θ_γ~0 is well known to be about 100nb/sr and the experimentally measured hypernuclear yields of $^{12}_\Lambda$B were used to estimate it for the new setup.

Although the expected yield for the new setup is about half of the previous Hall C experiment, the accidental rate is expected to be low for high Z targets since Bremsstrahlung is highly suppressed. The new configuration can provide a good signal to noise ratio as in the previous Hall A experiment and increases the hypernuclear yield rate by a factor of five.

The expected yield for the new setup was obtained as **0.56** $^{12}_\Lambda$B$_{g.s.}$ for 100μA, 100mg/cm^2 target starting from the Hall-C result and scaling from the Hall-A result gave a consistent result as shown in Table 2-III.

Using the estimated $^{12}_\Lambda$B$_{g.s.}$ yield rate, hypernuclear yields and background rates for various targets are summarized in Table 2-IV.

It was assumed that background originates from the accidental coincidence between K$^+$ and e' and the background spreads uniformly in the acceptance of the missing mass. The quasifree production cross section of K$^+$ and e' are in proportional respectively to $A^{0.8}$ which was estimated from the ^{12}C(γ,K$^+$) reaction and A which is expected in DIS region. All solid targets' thicknesses are normalized to be 100 mg/cm^2.

Table 2-III: Gain factor over the previous experiments and estimated production rate using the same luminosity.

Itemized gain factors by the new configuration	Over the previous Hall A experiment	Over the revious Hall C experiment
Integrated virtual photon flux ($\int\Gamma(E,E',\theta)dE'd\Omega$) per electron	2.16	0.91
K$^+$ survival rate	1.86	0.93
Integrated photo-production cross section ($\Delta\Omega_K$)	1.35	0.66
Beam current: 100μA	1	1
C target thickness: 100mg/cm^2	1	1
Total gain factor	5.42	0.56
Experimentally measured rate in E94-017, E05-115 (normalized to 100μA, 100 mg/cm^2)	10 counts/hr	100 counts/hr
Estimated count rate ($^{12}_\Lambda$B ground state 1$^-$ and 2$^-$ together) for new setup	54 counts/hr	56 counts/hr
Estimated count rate per (1.0 nb/sr)	0.54 counts/hr	**0.56** counts/hr

Table 2-IV: Expected hypernuclear production rates
 (100mg/cm^2 target thick for solid targets were assumed.)

Target	Beam curent (μA)	Produced Hyper-nucleus	HY yield per 100nb/sr per hour	Assumed Cross Section (nb/sr)	Hypernuclear Yield per hour	B.G. level in 1 MeV per hour	Signal to Accidental Background
Liq. ^{1}H (283mg/cm^2)	100	Λ	1915	580	11110	58	192
Liq. ^{4}He (500mg/cm^2)	10	Λ	85	12.4	10.5	1.4	7.6
^{12}C	100	$^{12}_{\Lambda}$B	56.4	100	56.4	4.4	12.8
^{27}Al	100	$^{27}_{\Lambda}$Mg	25.1	50	12.5	3.7	3.4
^{40}Ca	100	$^{40}_{\Lambda}$K	16.9	84	14.2	3.5	4.1
^{48}Ti	100	$^{48}_{\Lambda}$Sc	14.1	50	7.1	3.3	2.1
^{208}Pb	25	$^{208}_{\Lambda}$Tl	0.35	17	0.06	0.1	0.6

2.3 Expected mass resolution

Following factors contribute to the total mass resolution of the (e,e'K$^+$) experiment.

1. Spectrometers' momentum resolution.
    Since HKS (K$^+$) and HRS (e') are already established spectrometers, relative momentum resolutions are known.
2. Beam energy resolution.
    We assumed $dE/E < 5 \times 10^{-5}$ for 4.5 GeV electron beam.
3. Kinematic broadening due to uncertainty of the K$^+$ and e' scattering angles.
    The uncertainties of the K$^+$ and e' emission angles are originating from the multiple scattering through the materials between the target and tracking chambers in addition to the angular resolution of the spectrometer itself. This effect is significant for hyperon production or light hypernuclei, but less significant for heavier ones since recoil momentum of the hypernuclei is much smaller.
4. Energy loss and straggling in the target.
    Since our vertex resolution is not enough to determine the reaction point in the solid target (typically thickness is less than half mm while liquid target thick is 40 mm), so energy loss of charged particle can be corrected only as an average. Its distribution including straggling will contribute the final mass resolution. For kaon, both of energy loss distribution due to reaction point distribution and straggling will contribute while the sum of energy losses in the target for beam and scattered electron is roughly constant and thus only straggling is problem. These effects were estimated with GEANT simulation.

 Assumed parameters are: E$_B$ = 4.5GeV, P$_K$ = 1.2 GeV/c, P$_{e'}$ = 3.0 GeV/c, target thick of 100mg/cm^2 except for hydrogen and helium. Random contributions of 1-3 and straggling are quadratically summed and energy loss distribution in the target was convoluted to estimate the final mass resolution.

Table 2-V: Expected mass resolution for various targets (100mg/cm^2 target thick)

Target	Liq. ^{1}H (283 mg/cm^2)	Liq. ^{4}He (500mg/cm^2)	^{12}C	^{28}Al	^{208}Pb
K spectrometer	190	190	190	190	190
e' spectrometer	300	300	300	300	300
Beam resolution	220	220	220	220	220
K, e' angles	400	380	150	170	130
Energy loss/straggling	610	560	230	155	140
Total	840	800	670	610	580

All units are in keV and FWHM. Energy losses in the liquid targets are considered to be corrected.

2.4 Calibration and detector commissioning

With septum magnets, HKS and HRS spectrometers are optically separated and individual calibration with elastic scattering will be performed. This is a well-established technique successfully used in Hall A. The spectrometer with septum is setup to observe elastic scattering off a heavy, usually Tantalum, target. A series of spectra are taken such that the elastic peak has various δ values. This is done by adjusting the magnetic fields of all components up or down by the same amount while leaving the beam energy constant. Further these elastic peak data sets can be taken with a sieve placed at the entrance to the spectrometer in order to calibrate the angular measurements and also with a segmented target to aid in vertex reconstruction. This will require about one shift at beam momentum close to the momentum to be used in each arm during the experiment.

Absolute missing mass scale calibration will be carried out with protons in a CH$_2$ target with a few nA electron beam by p(e,e'K$^+$) Λ, Σ^0 using the precisely known hyperon masses. The wide momentum acceptance of the HKS makes it possible to observe both the Λ and Σ^0 peaks simultaneously under the same conditions as the solid targets. This technique was also well-established in the Hall-C HKS-HES experiment.

2.7 Conclusion

The configuration designed for future hypernuclear physics experiments promotes high yield and clean spectroscopy. It makes possible a program to study elementary Λ production at $Q^2 \sim$ 0.2 (GeV/c)^2 , a range of small $\theta_{\gamma K\_CM}$ angles and the precise spectroscopy of hypernuclei from few-body systems to those as heavy as $^{208}_{\Lambda}$Tl. The energy resolution can be at a level of 600-800 keV (FWHM) depending on the target. In addition, the new configuration equips pion spectrometers so that the decay pion spectroscopy experiment can be run simultaneously.

Part 2.

The Study of Hypernuclei with the (e,e'K$^+$) Reaction

1. Elementary production of Λ

There are two important reasons to measure the elementary $^1H(e, e'K^+)\Lambda$ reaction:

- To measure the elementrary production cross section as input for hypernuclear calculations at the identical kinematics.
- To determine the small angle behavior of the angular distribution.

Calculations of the hypernuclear cross section use the elementary amplitudes and a hypernuclear wavefunction. By measuring the $^1H(e, e'^{K^+})\Lambda$ reaction at the identical kinematics, the comparison to theory using different wavefunctions (and therefore different hyperon-nucleon potentials) is cleaner and simpler. However the elementary reaction itself is also interesting in this kinematics region.
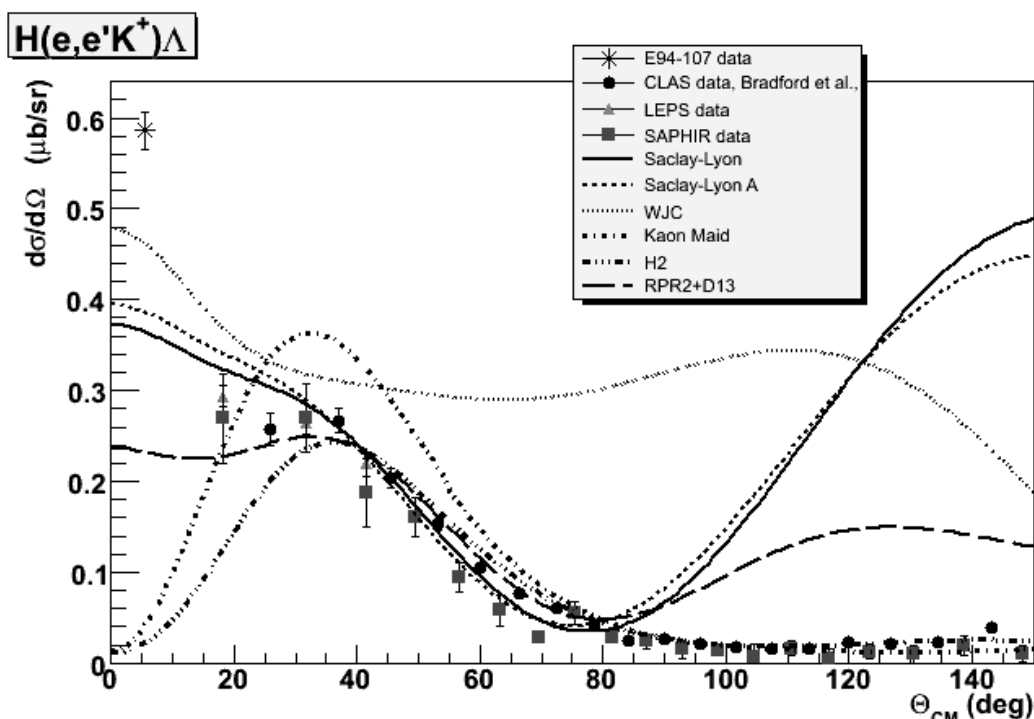
Fig. 1-1: E94-107 electroproduction result with Q^2 ~0.07 (GeV/c)^2, W=2.2 GeV and θ_{CM}=6° compared to photoproduction data and models, all of them with W=2.2 GeV. Error bars in E94-107 result represent total uncertainty (statistical and systematic uncertainties). CLAS data from Bradford et al.

The small angle behavior of the cross section is poorly known (see Figure 1.1, results from E94-107 running at higher W). Ideally the comparison would be to photoproduction however CLAS, SAPHIR and LEGS have difficulty reaching angles smaller than ~20°. This experiment will cover the range $\theta_{\gamma K} \approx 0°$ and allow for several bins. [The time for acquiring good statistics here is fairly short, but calibrations and systematic checks are important.] Additionally the ratio of

the $\Lambda : \Sigma^0$ final states is an interesting result. The isospin difference between the two final states leads to a simple prediction for the ratio of 3.7 in the quark model, although the isobar models have a range of predictions.

1.1 Physics Motivation

The photo- and electroproduction of kaon-hyperon pairs on nucleons in the resonance region can be described by the isobar [SLA96,JAN01,KM99] and Regge-plus-resonance [RPR06] models. These models consider only a single channel for the production process, neglecting couplings with the other channels in the final state, e.g. π or η production. More elaborate approaches in which all important channels coupled to the kaon photoproduction are simultaneously included [CHI01] are not suited for description of hypernucleus electroproduction due to their complexity.

Assuming exchanges of the nucleon, kaon, and hyperon resonances in the intermediate states in the isobar models can confirm the importance of a "missing" resonance and probe the resonance properties. Parameters of the model's effective Lagrangian (masses, coupling constants, and form factors) have to be taken either from other measurements or have to be fit to experimental data, usually photoproduction data (Q^2 =0) [SLA96,KM99,JAN01]. In electroproduction, longitudinal couplings of the virtual photon in the nucleon-resonance vertexes provide additional, new coupling constants which cannot be specifieded in photoproduction. The kinematical region of low Q^2 is important in determining the slope of the Q^2 dependence near the photoproduction point from which one can infer the importance of the longitudinal couplings and determine values of the coupling constants [ACH12]. This low Q^2 region has the minimal uncertainty due to the electromagnetic form factors (these form factors are not known well for the baryon and meson resonances).

The isobaric models differ from each other in their treatment of hadronic structure in the strong-interaction vertex. The Saclay-Lyon (SLA) [SLA96] model assumes point-like structure of hadrons whereas the Kaon-MAID (KM) [KM99] and Ghent isobar [JAN01] models include momentum dependent form factors in the strong vertexes. These hadronic form factors (h.f.f.) become important for a description of the process at photon lab energies larger than 1.5 GeV since they suppress the cross section as a function of energy. In the succesful SLA model, the suppression is realized by exchanges of hyperon resonances. The Williams-Ji-Cotanch (WJC) [WJC92] model, in which h.f.f. are not assumed and which includes only one hyperon resonance, overpredicts the photo-production cross sections for photon energies larger than 2 GeV. Due to the dynamical content of isobar models (tree-level, resonance masses smaller than 2 GeV) their validity is limited to photon lab energy from threshold up to 2.2 - 2.5 GeV.

In the Regge-plus-resonance model [RPR06], the background part of the amplitude is described by the Regge trajectory formalism fixed by high-energy photo-production data and the resonant part is modeled via exchanges of nucleon resonances fitted to the data in the resonance region. A set of relevant resonances were selected in the careful analyss is based on the Bayesian inference method. This model describes data from the threshold up to about 20 GeV.
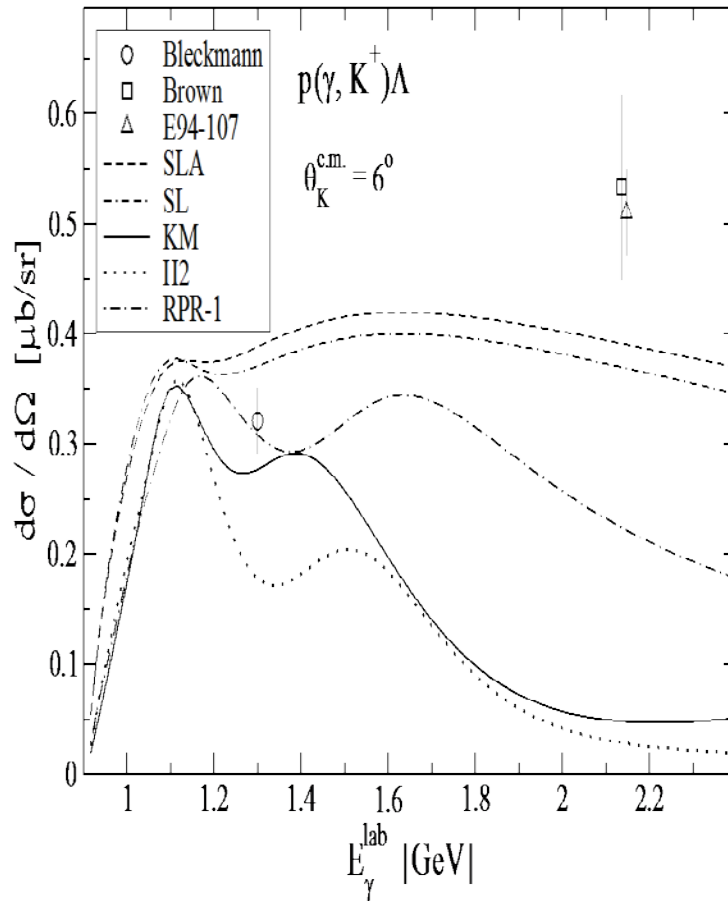

Fig. 1-2: Predictions of isobar (Saclay-Lyon: SL and SLA; Kaon-MAID: KM; and H2 [BYD03]) and Regge-plus-resonance (RPR-1 [BYD12]) models for the photoproduction cross section at kaon c.m. angle 6°. The data point 'Bleckmann' is for photoproduction and the points 'Brown' and 'E94-107' are for electroproduction with very small Q^2.

Due to a strong supression by nucleus-hypernucleus transition form factors, the cross sections for the electroproduction of hypernuclei are sensitive only to the elementary amplitude for very

small kaon angles. Obtaining reasonably large values of the hypernucleus-production counting rates also requires a small value of the virtual-photon mass (Q^2). Unfortunately, particularly in this kinematical region, dynamics of the elementary process are not well determined due to the lack of precision experimental data on the elementary photo- and electroproduction. In the region of small kaon angles and the photon lab energies larger than 1.7 GeV, the theoretical models reveal quite different predictions for the cross sections (see Fig 1-2) which then makes predictions for the hypernucleus cross sections unreliable.

Calculations of the cross section for production of hypernuclei in excited states, e.g. to analyze data from the hypernuclear experiments carried out in Jefferson Laboratory, depend on two main ingredients, the elementary-production operator and the nuclear and hypernuclear structure information. To learn more on the hypernuclear structure, which is closely connected with the hyperon-nucleon interaction, the uncertainty regarding the elementary process must be under control, at least in the relevant kinematical region. Presently however, predictions for the hypernuclear production cross sections using various isobaric models for the elementary operator differ by more than 100% for kaon laboratory angles less than 10 degrees and photon energies larger than 1.5 GeV. The best result for electroproduction of $^{12}_{\Lambda}$B hypernucleus was achieved with the SLA model [IOD07].

Precise measurements of the energy dependence of the cross sections in kaon electroproduction on the proton at a very small kaon angle would help in determining the dynamics of the process at forward kaon angles. Moreover, measurements performed at small values of the virtual-photon mass are important for the understanding of the process with the virtual photons, in the framework of an effective Lagrangian it means a better knowledge of the couplings of the virtual photon with baryon fields (the longitudinal couplings). The cross section of Λ production at low Q^2 and at a reasonably small forward angle for the kaon with respect to the virtual photon can be measured by this new experiment (with a setup similar to the Hall A 6 GeV experiments [E94-107, CUS09, IOD07, JOP11]) with much improved statistics. Similar studies have been performed by the Hall B CLAS for a wide range of high Q^2 and relatively large kaon CM angles. In this respect, the results from the new experiments would be complementary to existing data and would help in building a proper theoretical model. Consequently, the hypernucleus-production cross sections could be calculated more accurately. In addition, he helicity-dependent longitudinal-transfer interference term of the Λ electroproduction cross section can be measured by the asymmetry of Λ productions with two different beam helicities with a range of reaction angle, Φ. The interference terms being sensitive to details of the amplitude are therefore more constraining in model construction than the dominant transverse term. Moreover, at this moment the data on the separated cross sections are scarce and do not cover the kinematical region relevant for the hypernucleus electroproduction. At MAMI-C, the measurements of the interference terms are being performed now but the accessible energy at MAMI-C is smaller than the energy accessible at JLab. The data from JLab would be an extension of the results from MAMI [ACH12] to higher energies. The new experiment with a (4cm) liquid H_2 target can be done with good statistics in only a few days of beam time.

References

[SLA96] J.C. David, C. Fayard, G.-H. Lamot, B. Saghai, **Phys. Rev. C 53**, 2613 (1996);
T. Mizutani, C. Fayard, G.-H. Lamot, B. Saghai, **Phys. Rev. C 58**, 75 (1998).

[JAN01] S. Janssen, J. Ryckebusch, D. Debruyne, T. Van Cauteren, **Phys. Rev. C 65**, 015201 (2001).

[KM99] T. Mart and C. Bennhold, **Phys. Rev. 61**, 012201 (1999);
C. Bennhold *et al.,*nucl-th/9901066.

[RPR06] T. Corthals, J. Ryckebusch, and T. Van Cauteren, **Phys. Rev. C 73** (2006) 045207;
T. Corthals, T. Van Cauteren, J. Ryckebusch, D.G. Ireland, **Phys. Rev. C 75** (2007) 045204;
L. De Cruz, D.G. Ireland, P. Vancraeyveld, and J. Ryckebusch, **Phys. Lett. B694** (2010) 33;
L. De Cruz, T. Vrancx, P. Vancraeyveld, and J. Ryckebusch, **Phys. Rev. Lett. 108** (2012) 182002.

[CHI01] W.T. Chiang, F. Tabakin, T.-S.H. Lee, and B. Saghai, **Phys. Lett. B 517** (2001) 101;
G. Penner and U. Mosel, **Phys. Rev. C 66** (2002) 055212;
B. Julia-Diaz, B. Saghai, T.-S. Lee, F. Tabakin, **Phys. Rev. C 73** (2006) 055204;
R. Shyam, O. Scholten, and H. Lenske, **Phys. Rev. C 81** (2010) 015204.

[ACH12] P. Achenbach *et. al.*, **Eur. Phys. J. A48** (2012) 14;
P. Achenbach *et. al*., **Nucl. Phys. A 881** (2012) 187.

[WJC92] R.A. Williams, Chueng-Ryong. Ji, and S.R. Cotanch, **Phys. Rev. C 46**, 1617 (1992).

[BYD03] P. Bydžovský and M. Sotona, **Nucl. Phys. A 754 (2005)** 243c.

[BYD12] P. Bydžovský and D. Skoupil, **arXiv:1212.0337v1** [nucl-th].

[IOD07] M. Iodice *et. al.,* **Phys. Rev. Lett. 99**, 052501 (2007);

[E94-107] F. Garibaldi, S. Frullani, P. Markowitz, J. LeRose, **JLab Experiment E94-107**,(1994).

[CUS09] F. Cusanno *et. al*., **Phys. Rev. let. 103**, 202501 (2009).

[JOP11]   Chapter 13, "*New Insights into the Structure of Matter: The First Decade of Science at Jefferson Lab*," Editors: D. Higinbotham, W. Melnitchouk and A. Thomas, **Journal of Physics: Conference Series, 299** (2011).

2 Few-body systems

2.1 Charge Symmetry Breaking of the ΛN interaction

The Study of s-shell hypernuclei is mostly motivated by the study of the ΛN interaction since precise few-body calculation techniques are well established and it enables us to study the ΛN interaction with less ambiguity. So far, it has been commonly believed that the lightest Λ-nucleus system is $^3_\Lambda$H. However, , though it is not yet established [Sai12], there was an indication of Λn invariant mass enhancement over a large continuum background in an experiment using heavy ion collisions at GSI. In that experiment experimental resolution and calibration tools were limited. Thus, it is difficult to determine whether this is a Λn bound system, which was never found with intensive studies with kaon beams in the 80's. Obviously the momentum transfer in the heavy ion collision is higher than for the meson exchange reaction using a kaon beam. Since most of the theoretical models predict no Λn bound state, confirmation of the existence or the non-existence of this system should be clarified experimentally.

The system provides direct information about *ΛN* interactions. The $^4_\Lambda$H is a perfect few body system containing one Λ. With known wave functions for the Λ and the nucleons, the system can be treated exactly. Thus it is one of a few ideal few body systems, along with $^4_\Lambda$H and $^4_\Lambda$He, that can be used to test the basic understanding of the *ΛN* interactions. Since the current theoretical framework of the charge symmetry breaking (CSB) effect of the ΛN potential is phenomenologically implemented and it is based on the mass difference between $^4_\Lambda$H and $^4_\Lambda$He measured by emulsion experiments in the 60-70s, new measurements of A=4 iso-doublet hypernuclei with state-of-the-art counter techniques are necessary to clarify the CSB terms in the ΛN potential.
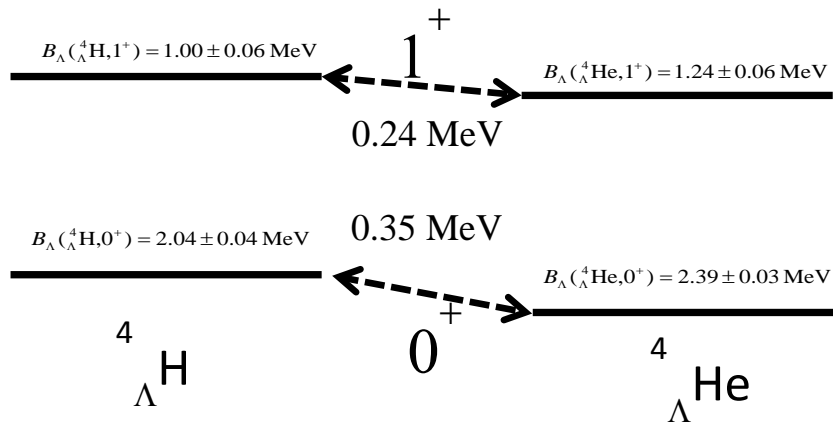

$B_\Lambda(^4_\Lambda\text{H},1^+) = 1.00 \pm 0.06\,\text{MeV}$

1^+

$B_\Lambda(^4_\Lambda\text{He},1^+) = 1.24 \pm 0.06\,\text{MeV}$

0.24 MeV

0.35 MeV

$B_\Lambda(^4_\Lambda\text{H},0^+) = 2.04 \pm 0.04\,\text{MeV}$

$B_\Lambda(^4_\Lambda\text{He},0^+) = 2.39 \pm 0.03\,\text{MeV}$

0^+

$^4_\Lambda\text{H}$

$^4_\Lambda\text{He}$

Fig. 2-1: Energy levels for ground and 1st excited states of A=4 hypernuclear doublet.

As shown in Fig. 2-1, the energy difference of $^4_\Lambda$H and $^4_\Lambda$ He ground states and 1st ground states are measured as a few 100 keV. The difference caused by Coulomb effects is expected to be at the 50keV level, therefore the mass difference between $^4_\Lambda$H and $^4_\Lambda$ He cannot be explained by Coulomb effects.

For normal nuclei, the binding energy difference between ^{3}H and ^{3}He after Coulomb correction is only 70 keV. The ΛN CSB effect for $^{4}_{\Lambda}$H and $^{4}_{\Lambda}$He is much larger than for the NN case.

Possible origins of a large ΛN CSB effect were discussed by [Gal66] and [Gib72], where the importance of the $\Lambda\Sigma$ coupling in the ΛNN three-body force was pointed out (Figure 2-2).
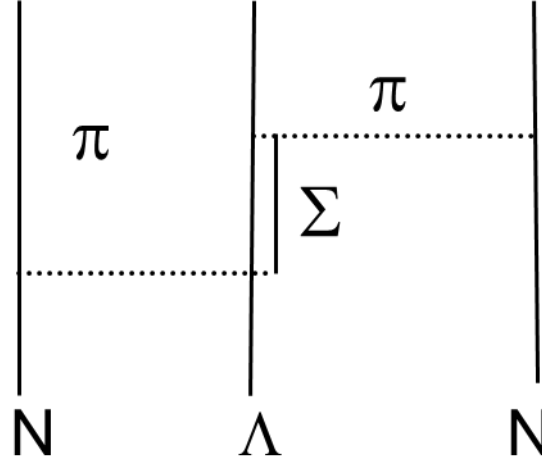

Figure 2-2: $\Lambda\Sigma$ counpling in the ΛNN three-body force

The mass difference between Σ and Λ is only 80MeV while for NΔ it is almost 300MeV, therefore, large mixing of the Σ is expected for ΛNN.

Furthermore, $\Sigma^{+,0,-}$ masses differ (eg. m(Σ^{+})-m(Σ^{-}) ~ 8MeV), but $\Delta^{++,+,0,-}$ masses are almost the same. So, CSB of ΛN is naturally larger than NN.

Although a very precise Fadeev-Yakubovsky calculation [Nog02] was carried out with $\square\Sigma$'s admixture, a consistent understanding of the $0^{+},1^{+}$ states of $^{4}_{\Lambda}$H and $^{4}_{\Lambda}$He has not yet been obtained.

The ground state energies of A=7 hypernuclear iso-triplet, $^{7}_{\Lambda}$He which was recently measured by (e,e'K^{+}) reaction at JLab [Nak13], $^{7}_{\Lambda}$Li* and $^{7}_{\Lambda}$Be were compared to a four-body cluster calculation (αNNΛ) [Hiy90] with and without inclusion of a phenomenological CSB potential.

Though the phenomenological CSB potential was originally introduced to explain Λ's binding energy difference of A=4 hypernuclear iso-doublet, $^{4}_{\Lambda}$H and $^{4}_{\Lambda}$He, inclusion of it makes the agreement between experimental results and theoretical prediction worse.

This implies that the current phenomenological CSB potential is too naïve or the starting point of this discussion, emulsion data of $^{4}_{\Lambda}$H and $^{4}_{\Lambda}$He, needs to be checked. The excitation energy of $^{4}_{\Lambda}$He will be measured with a Ge-array (Hyperball) at J-PARC, and the decay pion spectroscopy for $^{4}_{\Lambda}$H in this proposal determining the precise binding energy of the $^{4}_{\Lambda}$H ground

state and the ${}^{4}\text{He}(e,e'K^{+})$ ${}^{4}_{\Lambda}\text{H}$ reaction measures the binding energies of the ground and 1st excited level.

Since the excitation energy of the 1^{+} state of ${}^{4}_{\Lambda}\text{H}$ is only 1.04 MeV, a complete separation of the 0^{+} and 1^{+} states is difficult even for the high resolution (e,e'K) spectroscopy. Fig.2-3 shows an expected spectrum for 0^{+}, 1^{+} states of ${}^{4}_{\Lambda}\text{H}$ assuming 0.8MeV resolution and peak counts of 500 and 200 events for 0^{+} and 1^{+} peaks, respectively.
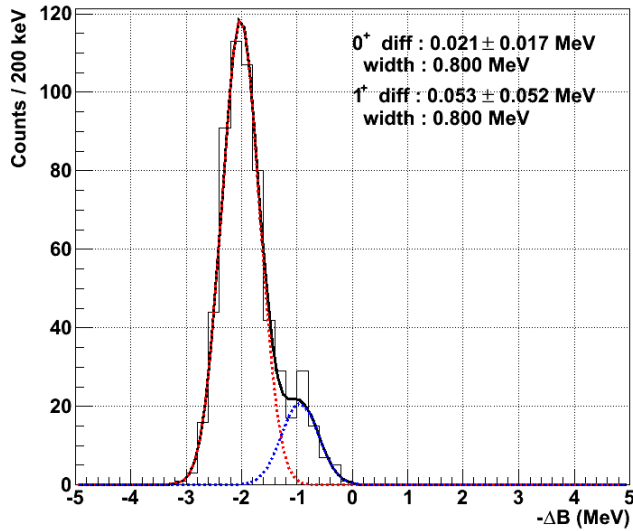

Figure 2-3: Expected spectrum for 0^{+} and 1^{+} states of ${}^{4}_{\Lambda}\text{H}$. 500 and 200 counts of 0^{+} and 1^{+} are assumed, respectively.

Fig. 2-4 is the result of a Monte Carlo study with various peak counts for the 1^{+} peak and constant background. If we have 500 counts for 0^{+} and more than 180 counts for 1^{+}, 100 keV accurary of the 1^{+} states's binding energy can be achieved if signal-to-noise ratio is better than 1:1.
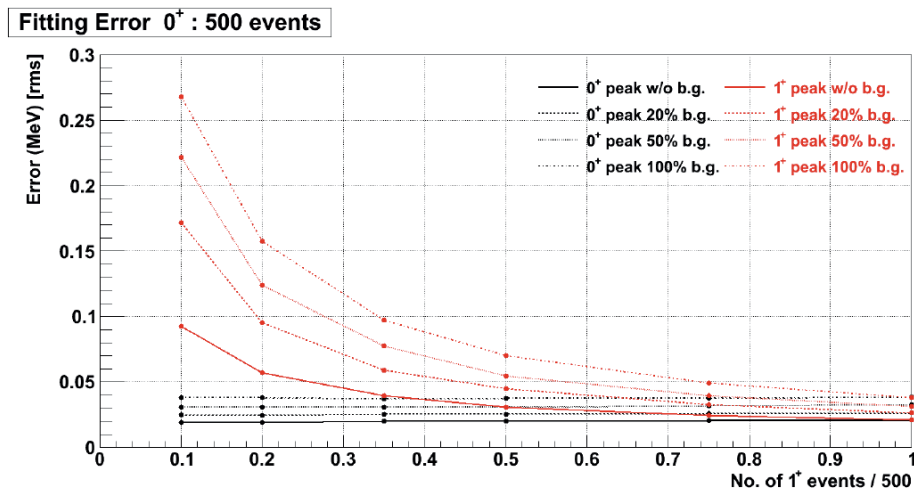

28

Figure 2-4: Fitting error for various numbers of events of 1^+ states of $^4_\Lambda$H and background levels. 500 counts of 0^+ were assumed.

Yield of $^4_\Lambda$H ground state was estimated with the production cross section of $^4_\Lambda$H as taken from E91-016 [Doh04] at 12.36 nb/sr for $\theta_{\gamma K}$=6 deg. in the photon-nucleus CM system. We scaled the counting rate for the elementary process from the $^{12}_\Lambda$B yield and normalized it to 500mg/cm^2 (4cm long) of helium target with 10μA beam, then 1.9/h of $^4_\Lambda$H ground state can be expected. In this estimation, we assumed 20% of observed $^4_\Lambda$H belongs to the ground state.

In order to have 500 events in the $^4_\Lambda$H ground state as we assumed for the error estimation,

$$263\text{h} = 11 \text{ days of beam time}$$

is necessary.

References

[Sai12] T. Saito . **FB20 conference,** Kyusyu, (2012).
[Gal66] A. Gal, Phys. Rev. **152** (1966) 975.
[Gib72] B. Gibson, A. Goldberg, M.S. Weiss, Phys. Rev. **C 6** (1972) 741.

[Nog02] A. Nogga, H.Kamada and W. Glˮockle, Phys. Rev. Lett. **88** (2002) 172501.

[Nak13] S.N. Nakamura *et al. (HKS-HES collaboration)*,

[Hiy09] E. Hiyama *et al.*, Phys. Rev. **C 80** (2009) 054321.

[Doh04] F.Dohrmann et al., Phys. Rev. Lett 93 (2004) 242501.

3. Medium heavy hypernuclei

As a natural extension of the successful hypernuclear programs at JLab, we propose a comprehensive study of hypernuclei in medium-heavy mass region as a part of a future program at JLab.

High-quality medium heavy hypernuclear masses will clarify the single-particle behavior of a Λ hyperon in the nuclear system, investigation of baryonic many-body system with strangeness degree of freedom, and the effective Λ-N interaction and *ls* splitting in the heavier hypernuclei beyond the p-shell. The experiment will take full advantage of the high quality electron beam of JLab.

3.1 Physics with beyond p-shell hypernuclei

In the investigation of hadronic many-body systems with strangeness, there is a fundamental question, "to what extent does a Λ hyperon keep its identity as a baryon inside a nucleus?" [Yam84]. Spectroscopic data in heavier hypernuclei can help to answer this question. Indeed, the relevance of the mean-field approximation in nuclear physics is one of the prime questions related to the role that the sub-structure of nucleons plays in the nucleus. The mean-field dynamics dominates the structure of medium ($A \geq 16$) and heavier ($A \geq 40$) nuclei and Λ hypernuclei prove the existence of single-particle motion from the deepest s-orbit up to large L valence orbits. The existing data from (π^+, K^+) reactions obtained at KEK, however, do not resolve the fine structure in the missing mass spectra due to limited energy resolution (a few MeV), and theoretical analyses suffer from those uncertainties. The improved energy resolution (500 ~ 800keV) of (e,e′K$^+$) hypernuclear spectroscopy, which is comparable to the spreading widths of the excited hypernuclear states, will provide the following:

- The mass (*A*) dependence of the central binding potential depth from the absolute Λ binding energies,
- Information about the spin-orbit splitting as a function of the core nucleus mass,
- Differentiation between the effects of the static spin-orbit potential and dynamical self-energies due to core polarization,
- Self-consistent interaction parameters for non-relativistic Hartree-Fock or relativistic mean-field theories.
- Access to collective motion of the core nucleus, namely deformation of the core nucleus, utilizing the Λ as a probe.
- Modify energy levels of a core nucleus by adding a Λ as an impurity.

Effective masses of a Λ hyperon in the nuclear potential will be obtained, which appears to be closer to that of the free value in contrast to the case of ordinary nuclei. Therefore, the proposed precision measurement of the single particle levels can address the degree of non-locality of the effective Λ-Nucleus potential and also can be compared, for example, with the advanced mean field calculations based on the quark-meson coupling (QMC) model by Thomas et al. [Tsu98] and on DDRH by Lenske et al. [Kei00]. This can be related to the nature of the ΛN and ΛNN

interactions, and to the ΛN short range interactions [Mot88]. In a more exotic way, the binding energies were discussed in terms of the distinguishability of a Λ hyperon in nuclear medium, which will result in a different A dependence of the binding energy as suggested by Dover [Dov87].

Figure 3-1 shows that A dependence of the Λ single particle energies calculated by mean-field theories with various parameters [Tsu98,Kei06]. In the A → ∞ limit, i.e. infinite matter, the ambiguity due to parameters in the relativistic mean field theories becomes smaller and reliable experimental input from the light to medium-heavy region is quite important. One can see that the data already taken at JLab and the proposed experiments will provide high precision experimental data which cover a wide A region almost uniformly, $^{6,7}_{\Lambda}$He, $^{10,11}_{\Lambda}$Be, $^{12}_{\Lambda}$B, $^{16}_{\Lambda}$N, $^{28}_{\Lambda}$Al, $^{40}_{\Lambda}$K, and $^{52}_{\Lambda}$V.

In order to have, accurate binding energies, good energy resolution and reliable calibration are important. The resolutions of the existing data by the (π⁺,K⁺) reaction are a few MeV and mass scale calibration depends on emulsion data of $^{12}_{\Lambda}$C hypernucleus mass, while the (e,e'K⁺) data will have a half MeV resolution with accurate mass calibration using well-known hyperon masses. A reliable absolute binding energy will provide the precious parameters for those calculations.
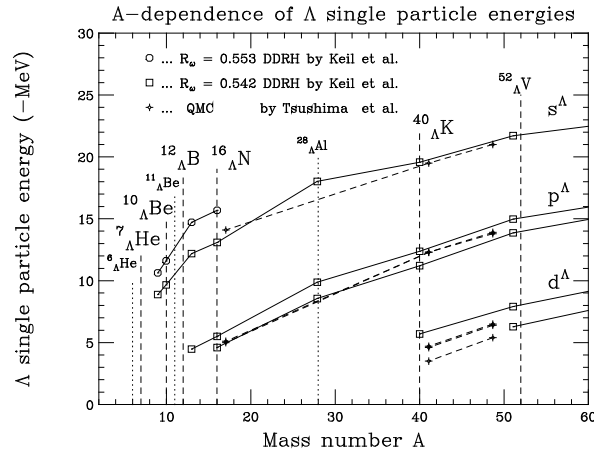

Figure 3-1: The calculated A dependence of Λ single particle energies of

$s_{\Lambda}, p_{\Lambda}, d_{\Lambda}$ states for various hypernuclei [Tsu98, Kei06]

We will also study the unique structure of medium-heavy Λ hypernuclei and possible spin-orbit splitting of the Λ single particle states in these hypernuclei.

The $^{89}_{\Lambda}$Y spectra taken by the (π⁺,K⁺) reaction show that the higher *l* states are split by about 1 MeV. These splittings are suggested to be due to the ΛN *ls* interaction, although the magnitude of the splitting is much larger than expected from previous measurements in the p-shell hypernuclei. The splitting was also interpreted as due to an interplay of different neutron hole states as suggested by a recent theoretical calculation [Mot08]. With a resolution of sub-MeV, we will try to disentangle closely degenerate hypernuclear states, and clarify the origin of the splittings. If the origin of the splitting is due to the *ls* interaction it will give us the magnitude of the interaction. If the splitting is due to core excitation, it will give us information on the

characteristic hypernuclear structure of medium-heavy hypernuclei. In either case, new features of Λ hypernuclei will be investigated.

The (e,e′K$^+$) hypernuclear study provides complementary and unique information to the existing meson induced hypernuclear experiments and future J-PARC experiments, since it converts a proton to a Λ. The elementary process of strangeness electro-production occurs on a bound proton and various hypernuclear states will be populated in the (e,e′K$^+$) reaction. Selecting an adequate target as a simple proton-neutron core, we can expect simple, but information rich excitation spectra for the electro-produced hypernuclei. The (e,e′K$^+$) spectroscopy has a chance to access the genuine hyperon interactions. Recent theoretical calculations for photo-production of ^{28}Si(γ,K$^+$)$^{28}_\Lambda$Al, ^{40}Ca(γ,K$^+$)$^{40}_\Lambda$K, and ^{52}Cr(γ,K$^+$)$^{52}_\Lambda$V were performed by Bydzovsky et al. [Byd12]. The spectra of those targets are expected to be simple and easy for analysis.

Especially $^{40}_\Lambda$K is clean, since the ^{40}Ca target is doubly LS-closed up to the 0d$_{3/2}$ shell. A precise mass spectrum of $^{40}_\Lambda$K will complete the A dependence of Λ single energies in the medium mass region.

Another interesting topic is that the Λ has the potential to study collective motion of the core nucleus. Triaxial deformation of ^{26}Mg as recently discussed and the special feature of the Λ's freedom from Pauli exclusion principle from nucleons will make it possible to prove the triaxial nature of ^{26}Mg.

Λ is considered to be bound to a core nucleus with weak-coupling and the core nucleus is not affected much by the existence of the Λ. However, in some cases, the Λ can affect the structure of the core and modify the energy level ordering. Measurement of a possible level modification about $^{48}_\Lambda$Sc hypernucleus is proposed. It is known that ^{45}Sc has degenerate ground states (7/2$^-$ and 3/2$^+$) with different deformations. There is a theoretical prediction that a Λ in an s-orbit couples to these state and the Λ's nature which is sensitive to deformation might separate the degeneracy. Similar phenomenon would be expected in $^{48}_\Lambda$Sc and that the Λ affects negative and positive parity states in a different manner to separate degenerate states.

Hypernuclear spectroscopy is a quite powerful tool for the quantitative investigation of these basic questions of hadronic many-body systems.
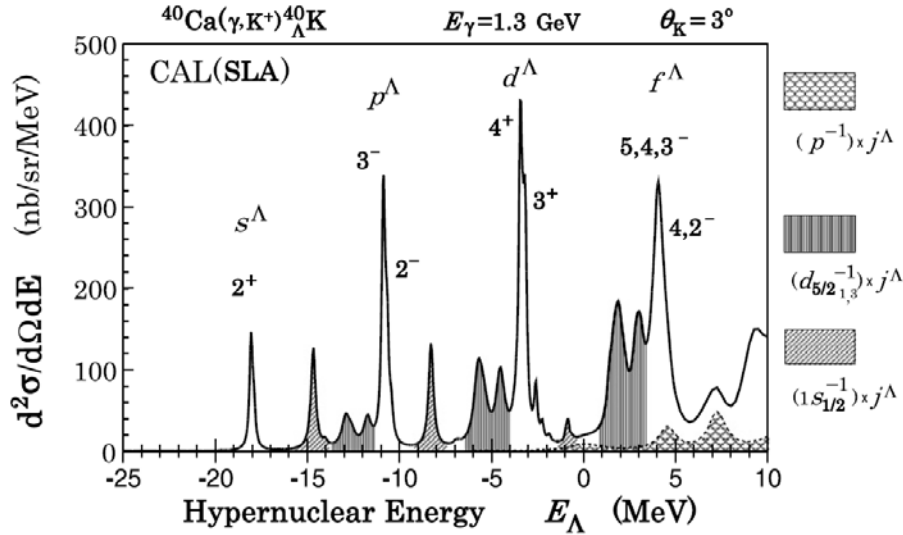
3.2 ^{40}Ca(e,e'K$^+$)$^{40}_\Lambda$K reaction

Figure 3-2: Calculated ^{40}Ca(γ,K$^+$)$^{40}_\Lambda$K excitation function by DWIA with SLA model. The calculation assumed $E_\gamma = 1.3$ GeV, $\theta_{\gamma K} = 3°$ and function *ls*-splitting of $0.17(2l+1)$ MeV [Byd12].

The ^{40}Ca target is doubly *LS*-closed up to the $0d_{3/2}$ shell. As shown in Figure 3-2, the ^{40}Ca(γ,K$^+$)$^{40}_\Lambda$K excitation function calculated by DWIA with SLA model [Byd12], $^{40}_\Lambda$K's natural parity states ($2^+,3^-,4^+$) are expected to be populated predominantly. Therefore, we can extract $s^\Lambda_{1/2}$, $p^\Lambda_{3/2}$ and $d^\Lambda_{5/2}$ energies from these peaks with less ambiguity.

For an *A*-dependence study of Λ single particle energies, it is important to have reliable $A = 40$ data to complete the systematic study of hypernuclei over a wide mass range, since we have data for $A < 10$ ^{6,7}Li, ^{10,11}B; $10 < A < 20$ ^{12}C, ^{16}O; $A \sim 30$ ^{28}Si; and $A \sim 50$ ^{52}Cr, only the A $\sim$ 40 target is missing up to $A \sim 50$.

Another interesting feature of a Ca target is the variety of isotopes. ^{40,44,48}Ca targets are available and their charge radii have interesting features. Usually, a larger charge radius can be expected for a nucleus with a larger mass number. However the charge radii of Ca isotopes are $r(^{40}$Ca) $\sim r(^{48}$Ca) $< r(^{44}$Ca). This is an example that neutron number affects charge radius even though these calcium isotopes have the same proton number and neutron numbers of magic numbers (N = 20,28) make the system tighter. The Ca(e,e'K$^+$)$_\Lambda$K reaction will enables us to study Λ hypernuclear isotopes systematically for the first time.

In order to study the isotope effect, the Λ binding energies for ^{40}Ca and ^{44}Ca will be carefully compared. It is better to measure ^{48}Ca to make a complete isotope study, but priority is set to measure ^{40}Ca target to have clean spectrum and ^{44}Ca for the study isotope difference.

3.3 ^{27}Al (e,e'K$^+$)$^{27}_\Lambda$Mg reaction

It is known that collective deformation plays important role in sd-shell nuclei. Though direct experimental evidence has not been found yet, triaxial deformation is expected to appear in the ground state of ^{24}Mg and theoretical works were developed in association with the shell gaps N=Z=12 prolate and N=Z=14 oblate region in Nilson diagram [Koe88].

Recently, similar triaxial quadrupole deformation is predicted for ^{26}Mg [Hin11]. While the deformation of ^{24}Mg has been discussed for decades, discussion of ^{26}Mg is not yet clarified since Z=12 and N=14 favor different shapes, prolate and oblate, for protons and neutrons respectively.

Behavior of these triaxial deformed nuclei with a Λ was already discussed for:
$$^{25}_\Lambda\text{Mg} = \Lambda + {}^{24}\text{Mg} \quad \text{and} \quad {}^{27}_\Lambda\text{Mg} = \Lambda + {}^{26}\text{Mg [Mya11].}$$

Added Λ makes potential energy surface slightly softer along the triaxial degree of freedom, but the energy surface of the core nuclei will be not changed and triaxially deformed nature will be kept for hypernuclei.

So far, deformation property or collective motion of hypernuclei have not been studied well, it is an interesting new field of research.

Similar phenomenon, a Λ in p-shell coupled to deformed nuclei, was theoretically discussed for $^{9}_\Lambda$Be and $^{13}_\Lambda$C [Aue83], and experimental observation exists for $^{9}_\Lambda$Be, which is ^{8}Be + Λ (Fig. 4.4.3) . The ^{8}Be nucleus is prolate deformed and Λ in p-shell has large overlap, thus deeper bound when Λ's orbit is in parallel to $\alpha-\alpha$ axis while it has less bound when Λ is in perpendicular to $\alpha-\alpha$ axis.

The Λ's p-orbit in parallel to the symmetry axis is so-called genuin hypernuclear state (#3, #4 peaks in Fig. 3-3, right), since a normal nucleon cannot occupy this orbit due to Pauli exclusion but Λ can. An indication of these states was obtained at BNL-AGS at first [Pil91e] and confirmed at KEK-PS by ^{9}Be (π^+,K$^+$)$^{9}_\Lambda$Be reaction [Has98].

This feature of Λ hypernucleus can be used for study of triaxial deformed nuclei. As shown in Fig. 3-4, Λ in p-orbit has different bound energies depending on Λ's directions along symmetry axises of triaxial deformed nucleus. So far theoretical study was performed for $^{25}_\Lambda$Mg [Isa12] and three rotational bands couple with Λ in p-orbit are expected. Figures 3-5 (top) and (middle) show the expected energy levels when $^{25}_\Lambda$Mg is prolate and oblate deformed. Figures 3-5 (bottom) is one for triaxially deformed. Only when $^{25}_\Lambda$Mg is triaxially deformed, characteristic three bands will show up for Λ in p-orbit. Observing this feature, it can be clearly confirmed that $^{25}_\Lambda$ Mg hypernucleus is triaxially deformed. High resolution of (e,e'K$^+$) hypernuclear reaction spectroscopy will help identification of these bands.

Production of $^{25}_\Lambda$ Mg by electron beam is difficult due to lack of ^{25}Al target but we can produce $^{27}_\Lambda$Mg hypernucleus by the ^{27}Al(e,e'K$^+$)$^{27}_\Lambda$Mg reaction. Detailed calculation is now in progress [Isa13] but we can expect quite similar behavior for $^{27}_\Lambda$ Mg [Mya11].

Precise spectroscopy of $^{27}_\Lambda$ Mg with sub-MeV resolution would make clear triaxial deformed ^{26}Mg structure and characteristic hypernuclear states.
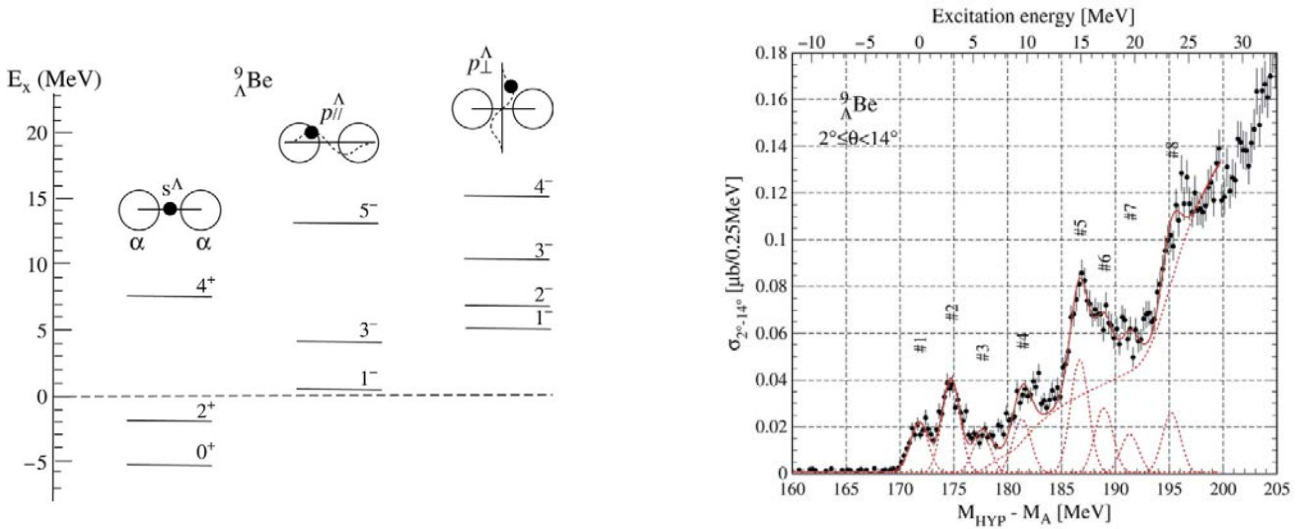
Figure 3-3: Energy levels of $^9_\Lambda$Be (left) and energy spectrum obtained by (π^+,K^+) reaction (right).

Large overlap leads deep binding

Middle

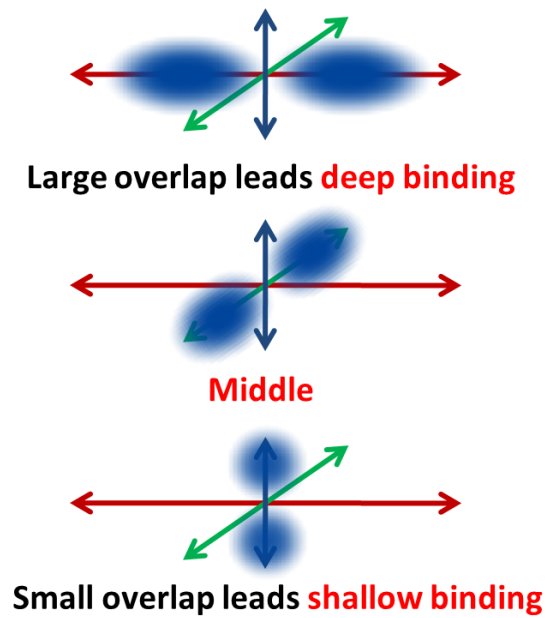**Small overlap leads shallow binding**

Figure 3-4: Conceptual picture when Λ in p-orbit overlaps three different symmetry axes of triaxial deformed nucleus.
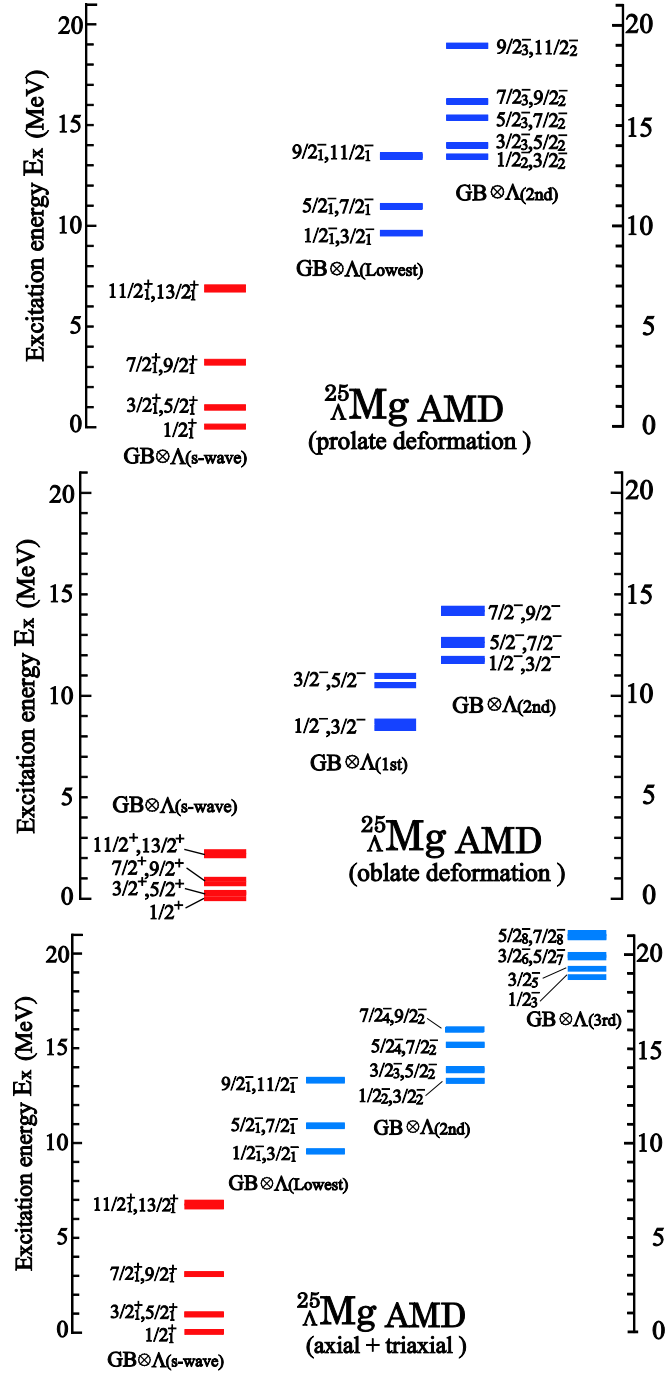
Figure 3-5: $^{25}_{\Lambda}$Mg energy levels for prolately, oblately and triaxially deformed cases.

3.4 ^{48}Ti (e,e'K$^+$)$^{48}_\Lambda$Sc reaction

Usually, Λ hypernuclei are treated as a system which a Λ is bound to a core nucleus in weak-coupling. Recently, it is discussed that Λ might affect the structure of core nucleus and thus energy levels' order of core nucleus and corresponding one of the hypernucleus are not necessarily the same. Those energy levels' inversions by adding a Λ, were discussed extensively by various theoretical approaches [Aue83, Hiy00,Isa11,Win08].

One of experimentally approachable examples of Λ's level modification is observation of Λ plus scandium isotope.
Ground states of ^{45}Sc (7/2$^-$ and 3/2$^+$) are degenerated ($\Delta E = 12.4$ keV), but their deformations are different. Recent AMD calculation pointed out a possibility that a Λ might separate these states by different ways of coupling to negative and positive parity states [Isaka].

Detailed calculation is in progress now for Sc isotopes and a preliminary result shows similar effect for $^{48}_\Lambda$Sc which can be produced by the ^{48}Ti(e,e'K$^+$)$^{48}_\Lambda$Sc reaction.

Fig. 4-6 shows preliminary calculation results for ^{47}Sc and $^{48}_\Lambda$Sc by AMD [Isaka]. Positive parity states (red, 3/2$^+$, 5/2$^+$) are pushed up by adding a Λ and level order between positive and negative parity states are changed.

The effect of adding a Λ to nuclear quadrupole-deformed nuclei would be a few 100~keV level of energy shift. It is difficult even for the (e,e'K$^+$) reaction to separate those states clearly, but sub-MeV resolution would serve to study such a slight shift using shape of the overlapped peaks with a help of theoretical predictions.
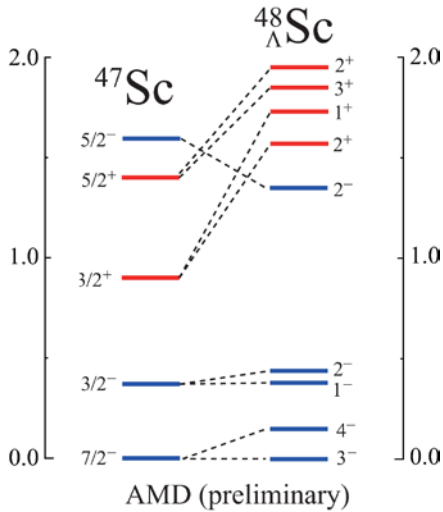

Figure 3-6: Preliminary calculation of energy levels for ^{47}Sc and $^{48}_\Lambda$Sc by AMD [Isaka].

4.5 Yield Estimation

Using yield estimation given in Chap1, Sec.2-2, expected hypenuclear production rates were summarized in Table 4-I.

In order to make statistical uncertainty to be less than expected missing mass calibration accuracy, we set goal of 40 keV statistical accuracy for the Λ binding energies assuming 700 keV missing mass resolution. In this case, each peak should have more than 300 counts.

Expected yield of ground states are 50-100 nb/sr, but we would like to study detailed structure of excited states, *eg*. Λ in p-orbit coupled to rotational bands of deformed core nucleus for the study of $^{27}_\Lambda$Mg case. Therefore, sensitivity of the experiment was set to 5-10 nb/sr which is smaller than most significant peaks.

Required beamtime for study of medium heavy hypernuclei to meet above goal was estimated as 806 hours. Including CH_2 target runs for absolute missing mass calibration and ^{12}C runs as a reference,

$$840 \text{ hours} = 5 \text{ weeks of beam time}$$

is requested for study of medium-heavy hypernuclei.

Table 4-I: Expected hypernuclear production rates (100μA beam, 100mg/cm^2 target thick)

Target	Produced Hyper-nucleus	HY yield per 100nb/sr per hour	Sensitive Cross Section (nb/sr)	Hypernuclear Yield per hour per sensitive cross section	B.G. level in 0.5 MeV per hour	Signal to Accidental Background S/N	Peak significance $\dfrac{S}{\sqrt{S+N}}$	Time to collect 300 counts (hours)
^{27}Al	$^{27}_\Lambda$Mg	25.1	5	1.3	1.8	0.70	10.3	240
^{40}Ca	$^{40}_\Lambda$K	16.9	10	1.7	1.7	0.99	10.5	178
^{44}Ca (^{48}Ca)	$^{44}_\Lambda$K($^{48}_\Lambda$K)	16.9	10	1.7	1.7	0.99	10.5	178
^{48}Ti	$^{48}_\Lambda$Sc	14.1	10	1.4	1.6	0.88	10.7	213

References

[Yam84] T. Yamazaki, *Proc. KEK Int. Workshop on Nuclear Physics in the GeV region*, KEK Report 84-20 (1984) 3.

[Tsu98] K. Tsushima, K. Saito, J. Haidenbauer, A.W. Thomas, *Nucl. Phys. A* **630** (1998) 691.

[Kai00] C.M. Keil, F. Hofmann, H.Lenske, *Phys. Rev. C* **61** (2000) 064309; H. Lenske, *presentation at HYP2006* (2006) Mainz.

[Mot08] T.Motoba, D.E.Lanskoy,D.J.Millener,Y.Yamamoto, *Nucl. Phys.* **A804** (2008) 99.

[Byd12] P.Bydzovsky, M.Sotona, T.Motoba, K.Itonaga. K.Ogawa and O.Hashimoto, *Nucl. Phys.* **A 881** (2012) 199.

[Mot88] T. Motoba, H. Bandˉo, R. Wünsch and J. Zofka, *Phys. Rev. C* **38** 1322 (1988).

[Dov87] C.B. Dover, *Proc. Int. Symp. on Medium Energy Physics*, Beijing, World Scientific, Singapore, (1987) 257.

[Koe88] W. Koepf and P.Ring, *Phys. Lett.* **B 212** (1988) 397.

[Hin11] N. Hinohara and Y. Kanada-En'yo, *Phys. Rev.* **C 83** (2011) 014321.

[Mya11] T.W. Myaing, K. Hagino and T. Koike, *Phys. Rev.* **C 83** (2011) 014301.
[Aue83] E.H.Auerobach et al., *Annal. of Phys*. **148** (1983) 381.

[Pil91] P.H. Pile *et al.*, *Phys. Rev. Lett.* **66** (1991) 2585.

[Has98] O.Hashimoto *et al.*, *Nucl. Phys..* **A639** (1998) 93c.

[Isa12] M. Isaka *et al.*, *Phys. Rev.* **C 87** (2012) 021304(R).

[Hiy00] E. Hiyama, *et al.*, *Phys. Rev. Lett.* **85** (2000) 270; E. Hiyama, *et al., Prog. Theo. Phys.* **128** (2012) 767; Y. Zhang, *et al., Nucl. Phys.* **A 881** (2012) 288.
[Isa11] M. Isaka *et al., Phys. Rev.* **C83** (2011) 054304.
[Win08] M.T. Win and K.Hagino, *Phys. Rev.* **C78** (2008) 054311.
[Isaka] M.Isaka, private communication

5 Spectroscopic study of heavy hypernuclei
^{208}Pb(e,e'K$^+$) $^{208}_\Lambda$Tl reaction

Abstract

The aim of this proposal is to study the ^{208}Pb(e,e'k) $^{208}_\Lambda$Tl reaction as an important part of a series of measurements the Jefferson Lab hypernuclear collaboration is proposing to this PAC. We will measure the Excitation Energy spectrum of the reaction in Hall A using the HRS spectrometer for electron and the HKS one for kaons. We will profit of the high quality Jlab electron beam, spectrometers and detectors setup that the hypernuclear collaboration contributed to improve for hypernuclear spectroscopy. We will use a pure Pb target cooled by cryogenic fluid that will allow to use 100 µA beam and a 100 mg/cm^2 target with reasonable yield and good energy resolution.The experiment will allow to extend the A range of the mass spectroscopy to its extreme. This is important for many reasons. Looking at deeply bound hypernuclear states in heavy hypernuclei has significance in investigating if a hyperon keeps his identity and is distinguishable as a barion in a nucleus. The mass dependence of the binding energy for each shell model orbital will be extended to A = 208, where the ambiguity in the relativistic mean field theories become smaller. ^{208}Pb was studied by means of the (π,K) reaction. The shell structures are barley visible because of the poor energy resolution that doesn't allow to resolve the spectral fine structure, introducing uncertainties into theoretical analyses. The good energy resolution of the (e,e'K) reaction will allow much more precise Λ single-particle energies to be determined providing complementary information with respect to what has been done in the past (and will be done at J-PARC) with hadron probes. Several theoretical model exist, new microscopic, ab initio, calculation that include explicitly three body forces become available. Their role can be tested comparing these calculation with standard mean field calculation. Moreover ^{208}Pb is the ideal target to study hyperons in medium resembling neutron star matter. Calculations of the mass-radius relation of stable neutron stars using G-matrix perturbation theory show that including the effects of three body YNN interactions lead to a large increase of the maximum mass. So a precise knowledge of the level structure can, by constraining the hyperon-nucleon potentials, contribute to more reliable predictions regarding the internal structure of neutron stars and in particular their maximum mass.

1. Introduction

The independent single particle picture of the nucleon is assumed as a basic principle of nuclear physics, but how well it holds? (e,e'p) experiments, among others, showed that the shell model of normal nuclei works fine for levels near the Fermi surface, but it does not guarantee that the shell orbits still exist deep inside of a nucleus, since direct observation of such states of a normal nucleus is practically impossible. Deviations from independent particle motion for orbits near the Fermi surface are clearly present and are attributed to various correlations leading to a sizeable depletion of the quasi particle states. Spectroscopic factors and occupation probability are basic elements for our understanding of the nuclear structure, measuring the accuracy of the shell model that is based on the mean field approximation. Experimental data show that these quantities are smaller than expected showing the limits of the mean field description of the nucleus.

On the other hand hypernuclear spectroscopy with the (π, K) reaction for the medium to heavy mass region established that the Λ keeps its identity even deep inside of a nucleus by observing clear s_Λ, p_Λ, d_Λ ... peaks and it provides a reasonable base for the independent particle (baryon) picture deep inside of nuclei [3,4]. This is as one expects if the Λ is a distinguishable particle not subject to the Pauli principle when added to nucleons, despite the fact that the baryons have quarks in common.

In heavy Λ-hypernuclei, a bound hyperon could be well inside the nucleus free from surface effects. Investigation of deeply bound hypernuclear states in heavy hypernuclei has significance in investigating if a hyperon keeps its identity and is distinguishable as a baryon in a nucleus. This, according to Dover [2], could be studied by means of the A dependence of the binding energy

The mass dependence of the binding energy for each shell model orbital should testify to the validity of a potential to describe hypernuclear states.
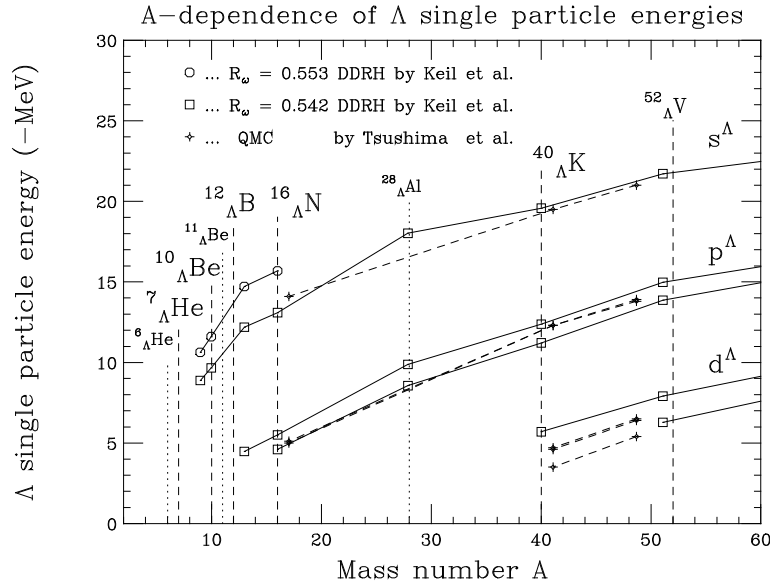
A–dependence of Λ single particle energies

Fig…. The calculated A dependence of Λ single particle
energies of s_Λ,p_Λ,d_Λ states for various hypernuclei [Ref...]

Fig… shows the A dependence of Λ single particle energy calculated by mean-field theories with various parameters [Ref..]. In the $A \rightarrow \infty$ limit, i.e. infinite matter, the ambiguity due to parameters in the relativistic mean field theories becomes smaller and reliable experimental input from the light and medium/heavy region is quite important. This is part of another proposal of the Jlab hypernuclear collaboration to this PAC. The key role of extending these measurements as far as possible in mass number (subject of the present proposal) is evident.

The depth of the potential felt by a Λ hyperon can be better determined from the single-particle levels of heavy Λ-hypernuclei, since only a few Λ orbitals are bound in light hypernuclei and information on the Λ potential is limited.

The Jlab hypernuclear collaboration performed successfully spectroscopic studies of light nuclei and is presenting proposals to study few body and medium mass nuclei to this PAC. A systematic study of Λ hypernuclear bound states over the wide mass range would deepen our understanding of the nature of the ΛN and ΛNN interactions in nuclear medium.

This study will allow one also to better constrain the current models of the Λ-Nucleon potential, which are at the basis of microscopic calculations of the equation of state of high density hadronic matter.

In this framework spectroscopic investigation of heavy Λ hypernuclei has unique importance.

The heavy hypernuclei have small cross sections for their inner shell–levels as seen in meson beam production, while the cross sections of higher orbital levels are relatively larger.

The clean extraction of Λ single-particle from (π,K) or (e,e'K) reactions requires a filled shell of high-j neutrons or protons, respectively, near the Fermi surface. This is because the cross section is proportional to the number of nucleons in the shell the high momentum (angular momentum) transfer permits the population of all

bound Λ orbits with a wide range of orbital angular momentum values. Closed shells for the other kind of nucleon makes for maximal symplicity of the level structure and the observed spectrum. Thus, the obvious choice for the heaviest target is the doubly-magic ^{208}Pb nucleus. Moreover data from (π,K) as well as from several (e,e'p) experiments exists [3,5,6,22]. In addition, it should be noted that the Λ-N particle-hole matrix elements are very small for heavy nuclei and that the level shifts and redistribution of strength due to configuration mixing will not lead to observable effects, even with the good resolution possible for the (e,e'K) reaction.

New microscopic MCarlo calculation are available [1, 23]. These calculations show that the inclusion of explicit ΛNN terms provides the necessary repulsion to realistically describe the separation energy of a Λ in hypernucley on intermediate and high masses [1]. As underlined in the introduction, accurate *ab initio* calculations (AMDC [1]), based on two-body potentials describing YN scattering data, showed these studies failing to simultaneously reproduce all the experimental separation energies, thus suggesting that three-body interactions involving nucleons and hyperons may have sizable effects [42]. The important role played by YNN forces in determining the Λ separation energies in a variety of nuclei with $5 \leq A \leq 91$ has been recently confirmed [1]. Combining the results of the AFDMC studies and the existing models of the ^{208}Pb spectral function, the formalism successfully employed to describe the (e,e'p) cross section can be readily generalized to the case of Λ electroproduction.

^{208}Pb was studied using the (π$^+$, K$^+$) reaction and the shell structures are barely visible [3]. The main reason was poor resolution (> 2MeV FWHM). This resolution is larger than the 1.8 MeV spacing between the 0i13/2 and 0h9/2 neutron hole states that produce two series of strongly populated states with the Λ in different orbits. In addition, the spacing between Λ single-particle states is only 4 to 6 MeV. As a result, the existing data do not resolve the two series of states, introducing uncertainties into the theoretical analyses.

The experiments we propose can have good statistics and sufficient resolution to separate at least the major shell states from those configuration mixing states as seen in the Hall C $^{28}_{\Lambda}$Al spectrum [12,13,15]. The more accurate information on the binding energies and spacing of the Λ single-particle states in heavy nuclei will provide an anchor point for the systematics of Λ single-particle states across the periodic table.

The study of ^{208}Pb with the (e, e'K$^+$) reaction will give better resolution and thus a more detailed understanding of baryon behavior deep inside of the nucleus. Such a high precision measurement may reveal how well the independent particle picture holds providing important information for studying the Λ single-particle nature under high nucleon density and testing descriptions by tmean-field theories.

Moreover, ^{208}Pb is the ideal target to study hyperons in a medium closely resembling neutron star matter. This environment is best suited to the investigate the effects of three body forces involving hyperons [1,21,22], which are believed to increase the stiffness of the nuclear matter equation of state, thus allowing for the existence of massive neutron stars compatible with the observational constraints.

As pointed out in the general introduction, hyperon production in the neutron star interior is believed to become energetically favored at around 2-3 times nuclear saturation density, and its occurrence may also signal the presence of a non-hadronic phase, i.e. of deconfined quark matter, in the inner core of the star.

The achievement of a better understanding of the the above issue will require accurate theoretical calculations, carried out within advanced many-body approaches based on realistic models of the baryon-baryon interactions.

In this context, three body forces involving hyperons are expected to play a pivotal role.

This point is illustrated in Fig. 1, showing the mass-radius relation of stable neutron stars obtained in **Ref. [?]** using G-matrix perturbation theory. The curves labeled 1 and 2 correspond to matter consisting of nucleons only, with and without inclusions of three-nucleon forces, respectively. The curve labeled 3 corresponds to matter including hyperons interacting with nucleons trough two-body, YN, forces only, while the curve labeled 4 has

been obtained taking into account the effects of three-body YNN interactions. It clearly appears that the inclusion of YNN forces leads to a large increase of the maximum mass, although the resulting value is still below the two solar mass line.
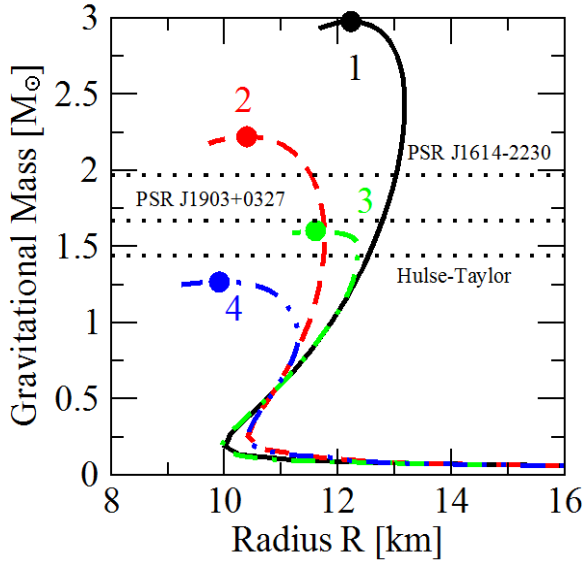

Fig. 1 Mass radius relation of stable neutron stars (see text)

In conclusion, even if the typical baryon density inside a neutron star is much higher than in a hypernucleus, a precise knowledge of the level structure can, by constraining the hyperon-nucleon potentials, contribute to more reliable predictions regarding the internal structure of neutrons stars, and in particular their maximum mass.

2. Proposed measurement

The aim of the experiment is measuring the ^{208}Pb(e,e'k) ^{208}Tl reaction. Fig 2 shows the missing mass spectrum obtained by the ^{208}Pb $(\pi,K)^{208}_{\Lambda}$Pb experiment [4]. It shows a characteristic bump structure starting from the binding energies B_{Λ} around 25 MeV. As explained in the previous section,   two series of states with the Λ hyperon coupled to the high-j neutron hole states near the Fermi surface are expected to be strongly populated but cannot be completely resolved. The binding energies of Λ hyperons were derived assuming they correspond to the peak centroids of the bumps. Altough the binding energies may depend on detail of the bump structures, the centroid values can be reasonably well deduced form the fitting [4]. Binding energy have been measured with the same reaction in several other nuclei, light and medium mass [3] to study its mass dependence also to get information about the distinguishability of the Λ hyperon in the nucleus [2]. The observed spectra were found to be significantly smoother than theoretical calculations [3,4].

The observed spectra were found to be significantly smoother than theoretical calculations [3,4]. "Therefore is of vital importance to perform precision spectroscopy of heavy Λ hypenuclei with mass resolution comparable to or better than the energy differences of core excited states, in order to further investigate the structure of the Λ hyperon deeply bound states in heavier nuclei. (e,e'K) spectroscopy is a promising approach to this problem"[3].

Spectroscopic data exist for few Λ hypernuclei also for (e,e'K) spectroscopy and few others would be available with the presently proposed experiment. Consequently is extremely important to perform (e,e'K)

experiment also on ^{208}Pb. The much better energy resolution of the (e,e'K), a factor of ~ 3 with respect to (π,K), will allow much more precise Λ single-particle energies to be determined.

This will allow us to extend the A range in the study of the mass dependence of the Λ binding energy. Measurements of the Lambda binding energy have been already performed with the (e,e'K) reaction in Hall A and Hall C reaction on several nuclei including the nominally doubly-closed shell nucleus ^{16}O. Measurements are proposed to this PAC on medium mass nuclei and Pb.

This will make possible to determine with much better precision the binding energy (calibration with hydrogen), and to test different theoretical models: relativistic mean field calculations, calculations using three-body ΛNN forces and Λ effective mass in the Skirme Hartree Fock approach [35,36], and the new microscopic MonteCarlo calculations [1]).

It will be possible to "see" deep shells, in practice not visible with (π,K) reaction ("the observed small peaks *are assumed* to be the sΛ states" [4]")

$$^{208}\text{Pb}(\pi^+,\text{K}^+)_\Lambda^{208}\text{Pb}, \text{ p}_\pi = 1.06 \text{ GeV/c}$$
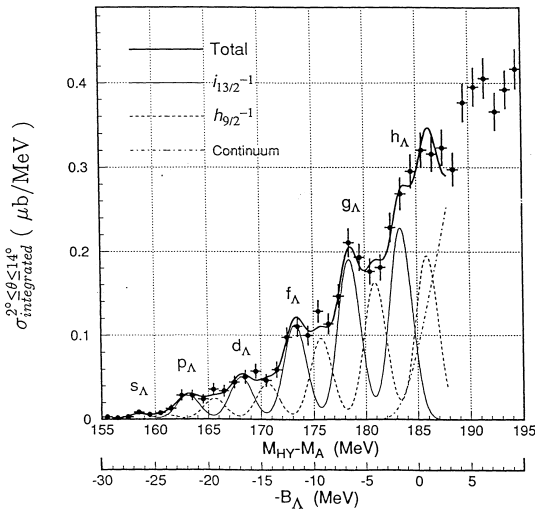
Fig. 2 Missing mass spectrum of 208Pb measured in E140 experiment

Fig. 3 shows the ^{207}Tl core nucleus level scheme. Table 1 shows that the spectroscopic factors measured in ^{208}Pb(d,^{3}He)^{207}Tl reaction are large enough to many low-lying states of ^{207}Tl core nucleus (up to excitation energy approx. 4 MeV) and that the corresponding hypernuclear states with lambda coupled to these core states are populated.

Tab. 1. ^{207}Tl energy spectrum, dominant
configurations and
spectroscopic factors

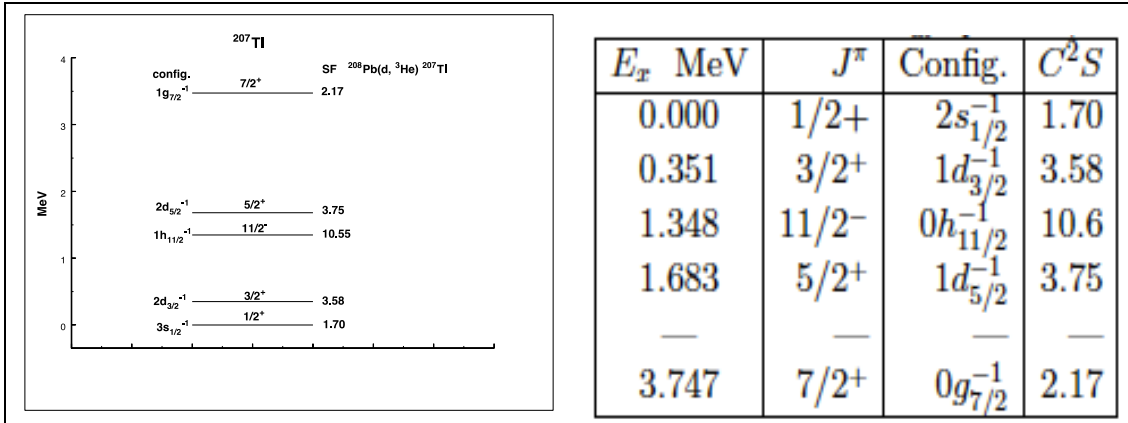| E_x MeV	J^π	Config.	C^2S
0.000	1/2+	$2s_{1/2}^{-1}$	1.70
0.351	3/2+	$1d_{3/2}^{-1}$	3.58
1.348	11/2−	$0h_{11/2}^{-1}$	10.6
1.683	5/2+	$1d_{5/2}^{-1}$	3.75
—	—	—	—
3.747	7/2+	$0g_{7/2}^{-1}$	2.17

Fig.3. ^{207}Tl core nucleus level scheme

Fig. 4 shows Spectrum for ^{208}Pb(γ,K+)$^{208}_\Lambda$Tl calculated for our kinematics using the SLA elementary amplitudes. The Λ is assumed to be weakly coupled to the proton-hole states of ^{207}Tl strongly populated in (e,e'p) or (d,3He) reactions on ^{208}Pb. The Λ single-particle energies were calculated from a Woods-Saxon well fitted to energies derived from the ^{208}Pb(π,K+)$^{208}_\Lambda$Pb reaction. States based on the closely-spaced p 2s1/2^{-1} and p 1d3/2^{-1} states cannot be resolved (blue bars and curves). Likewise for the p 0h11/2^{-1} and p 1d5/2^{-1} states cannot be resolved (blue bars and curves). Likewise for the p 0h11/2^{-1} and p 1d5/2^{-1} states (red bars and curves). The successive red and blue peaks correspond to the population of the 0s, 0p, 0d, 0f, 0g, and 0h Lambda orbits. The green lines correspond to the noded 1s, 1p, 1d/2s, and 1f Λ orbits. The remaining (wiggley) curves correspond to strength based on deeper and fragmented proton-hole strength.
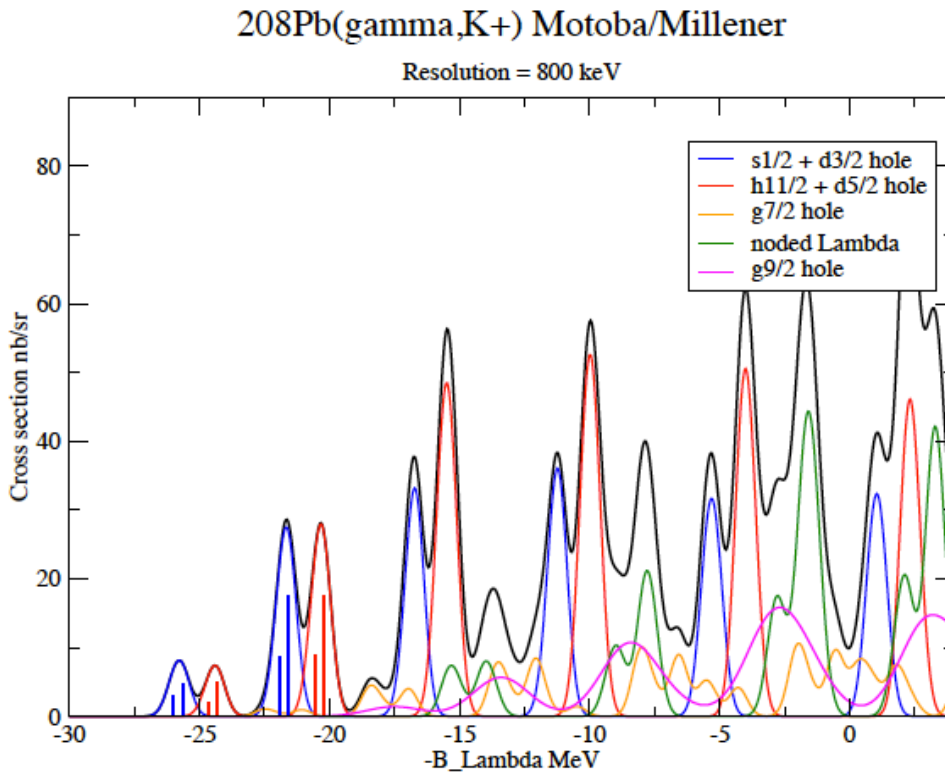

Fig. 4 Excitation energy plot (Millener Motoba calculation (see text)

The interpretation the results of the experiment that we are proposing should be quite straightforward. Earlier, it was noted that configuration mixing effects should be small and not produce observable effects in the spectrum obtained with a Pb target. The Motoba/Millener calculation shown in Fig.4 assumed weak-coupling of the Λ hyperon to the hole states of the core (i.e. no residual Λ–N interaction). This assumption can be checked by doing a simple particle-hole calculation with the Λ–N interaction that has been successful in describing the precision gamma-ray data obtained for p-shell hypernuclei. Then, one can extract Λ single-particle energies from each of the observed peaks. Each peak does correspond to several levels based on two closely-spaced proton-hole states. One has to rely slightly on theory for the centroid of these levels. The fact that one should get essentially the same energies from the peaks based on the two sets of pairs of hole states, separated by 1 MeV, provides a check on the assumptions made.

The main refinement to the Motoba/Millener calculation, which was performed using harmonic oscillator single-particle wave functions, is to repeat in using more realistic single-particle wave functions.

Once the Λ single-particle energies are known for Pb, many-body calculations using the Auxiliary Field Diffusion Monte Carlo (AFDMC) approach [1] can be used to try to determine the balance between the spin-independent components of the ΛN and ΛNN interactions required to fit Λ single-particle energies across the entire periodic table.

3. The target

A major concern is developing a Pb target that could operate at high beam currents without melting. We considered different options:.

a.   A 0.5 mm of Lead has to be sandwiched between two 0.15 mm of diamond that is pure ^{12}C as done by the PREX experiment [31] (see Fig. 5). This would allow to run with ~ 70 µA on a 100 mg/cm^2 (or thicker, but degradation of energy resolution would happen). The major drawback of this option would be the Excitation Energy spectrum highly contaminated by the Carbon spectrum.
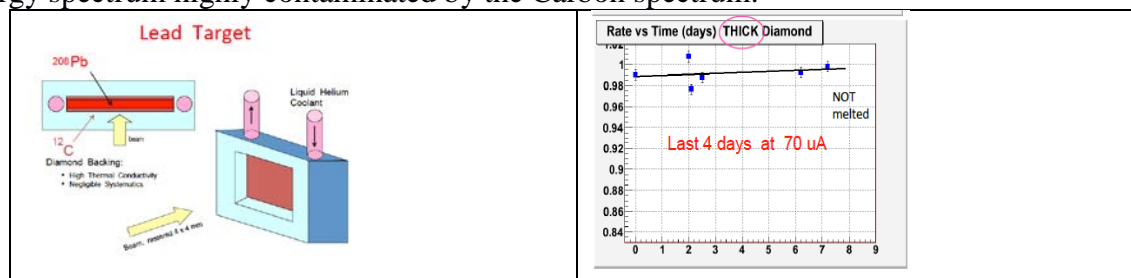
Fig. 5. The PREX Lead target.   Performance of one of the PREX targets

b.   The setup used at NIKHEF for (e,e'p) experiment [Ref. 6, and C. Marchand, personal communication]. This would allow to run safely with 10 µA of beam current and 100 mg/cm2 (or thicker) of pure ^{208}Pb target

c.   The same setup but cooling with a cryogenic liquid to allow to use with higher beam currents (~ 25 µA) to be able to increase the counting rate so improving the "detectability" of the small peaks.

After considering the options b and c and discussing with Jlab target group, we decided to adopt the solution c.

The Fig. 6 shows the layout of the NIKHEF layout of the ~ 100 mg/cm^2 pure Pb target [6].

Fig. 6 The NIKHEF ^{208}Pb target layout
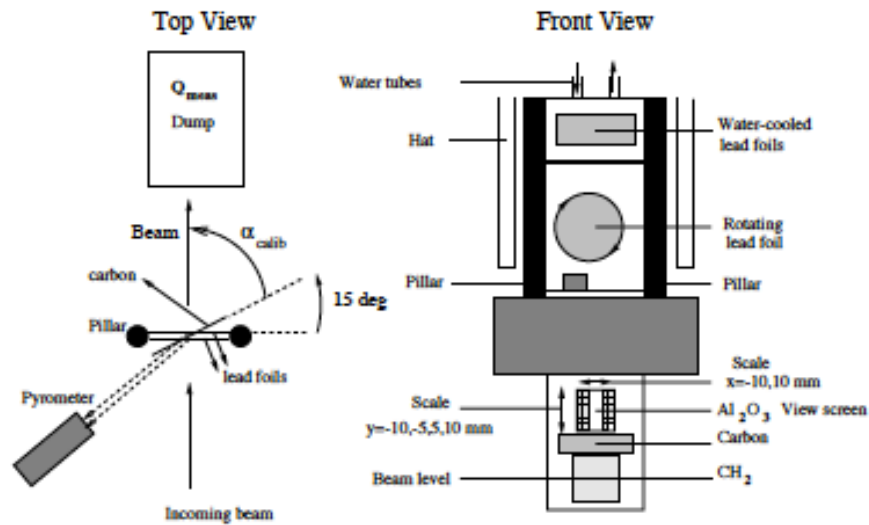
The beam current was 10 μA. To avoid melting the target was cooled by a water flow (15 °C) of up to 95 dm^3/h during the actual data taking.
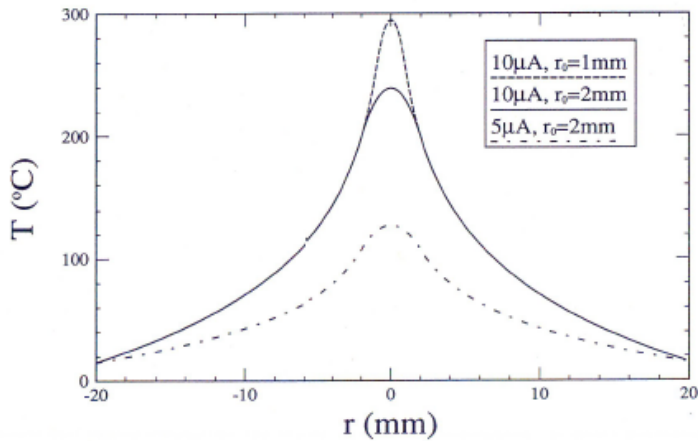
Fig.7. Temperature profile of a circular water cooled lead target of radius 20 mm. The dashed curve corresponds to 10 μA beam spot of 1 mm radius, the solid curve to a 10 μA beam spot of 2 mm radius. And the dot-dashed curve to a 5 μA beam spot of 2 mm radius.

Heat transfer calculation show that conduction cooling becomes competitive as compared to increased radiation cooling by rotating or wobbling the target for thick targets. The computed temperature profile caused by a beam spot of radius r_0 on a circular target of radius r_1 is shown in Fig. 7.

For our experiment we plan to use cryogenic fluid to cool the target. The maximum current one can use without melting the target can be calculated by the formula

$$<i_{max}> = 2\pi k \, (T_{melting} - T_0)/\{[\ln(r_1/r_0) + \tfrac{1}{2}] \, \rho dE/dx\}$$

where $<i>$ is the beam current, $k \sim 35.3 W.K^{-1}.m^{-1}$, $\rho \sim 11.35$ ⬜⬜⬜⬜ for lead, $T_{melting}$ is 601K for lead. This shows that using cryogenic cooling we can use a beam current at least of $\sim$ 25 μA. However, the actual

47

shape of the target is not circular, neither is the exact shape and size of the beam spot known. Therefore what shown in the Fig. 7 gives only a first order estimation of the expected heat dissipation performance.
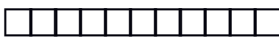
For this reason we will setup to setup a system that allows to monitor continuously the target thickness when is exposed to beam. At Nikhef the temperature was monitored by a pyrometer setup. This instrument measured a temperature of 394-414 K during the experiment which was conveniently below the melting temperature of lead (601 K). The position of this instrument is shown in Fig.6.

For our experiment we plan to monitor the target thickness by performing elastic scattering measurement off Pb-208 to know the actual thickness of the target at the first stage of the beamtime. During data taking, we will monitor continuously the thickness of the target by measuring electron scattering rate as a function of two-dimensional positions by using raster information. This method was already used for CH2 target in Hall-C hypernuclear programs and cracking or melting of the target were monitored to know right time for target exchange.

4. Particle Identification

The identification of kaons detected in the hadron arm together with a huge background of protons and pions is one of the major challenge of the experiment. To reduce the background level in produced spectra, a very efficient PID system is necessary for unambiguous kaon identification. In the electron arm, the Gas Cherenkov counters [33]give pion rejection ratios up to 10^3. The dominant background (knock-on electrons) is reduced by a further 2 orders of magnitude by the lead glass shower counters, giving a total pion rejection ratio of 10^5. The lead-glass shower counters and the gas Cherenkov are calibrated against each other.

The PID system in the hadron arm of HKS (see par. 2) is composed of: three planes of time-of-flight counters, two planes of water Cerenkov counters, and three planes of aerogel Cerenkov counters. The power rejection capability is:

- □□□□□□□□□π:K:p 10000:1:2000
- in the on-line trigger 90:1:90
- after off-line analysis it is 0.01:1:0.02
- so for π the rejection power is 10^6
- and for proton 10^5

The Hall A RICH detector will be added to improve the kaon identification if needed. The detector [27,28,29] was used successfully during the E-94-107 experiment providing a very good pion/kaon rejection at 2 GeV/c better than 1:1000 (corresponding to a pion/kaon angle separation of ~ 6.0 sigma) [27,28,29].

The layout of the RICH is conceptually identical to the ALICE HMPID design [34]. It uses a proximity focusing geometry, a CsI photocathode, and a 15 mm thick liquid Freon radiator. A detailed description of the layout and the performance of the detector is given in [23, 24, 25]. After the E-94-107 experiment the detector was upgraded to match the needs of the Transversity approved experiment (E06-011) to be able to identify kaons of 2.4 GeV/c. [30]. The upgrade extended the performance by means of a larger photon detector (a multiwire-multipad proportional chamber) and a longer proximity gap which improved the photon detection geometrical efficiency and the angular resolution, respectively.

Upgraded Proximity Focusing RICH @ JLab
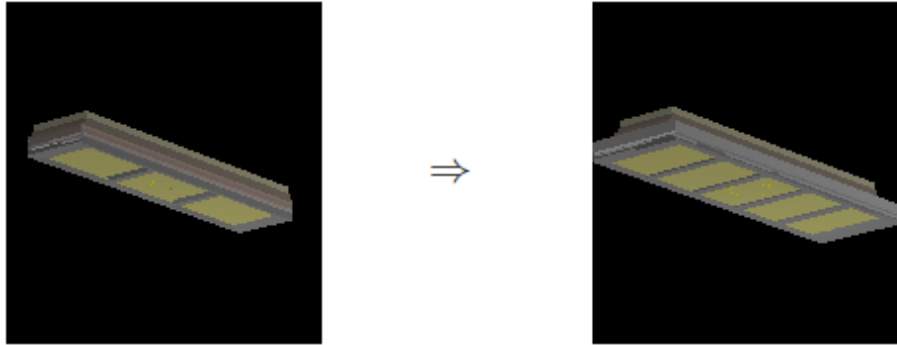
Radiator	15 mm thick Liquid Freon (C_6F_{14}, n=1.28)
Proximity Gap	100→ 175 mm, filled with Methane at STP
Photon converter	300 nm CsI film coated on Pad Planes
Position Detector	3→ 5 × pad planes = 1940 × 403→ 2015 × 646 mm^2
	Multi Wire/Pad Proportional Chamber, HV= 1050 ÷ 1100 V
Pad Plane	403.2 × 640 mm^2 (single pad: 8.4 × 8 mm^2)
FE Electronics	11520→ 19200 analog chs. multiplexed S&H

Fig. 8. Old and new upgrated RICH layout

In Fig. 8 we show the old and new (upgrated) layout. The photon detection plane was doubled (3 more pad panels added). This would have allowed the detectors to separate kaons, in the E-94-107 kinematical conditions (at a kaon momentum ~ 2 GeV/c) with a higher rejection ratio, an additional ~ 1.5 sigma (Fig.9) corresponding to a pion:kaon rejection better than 1:10000 at 2.0 GeV/c, with improved efficiency.

In our experiment the central momentum of the detected kaons will be 1.2 GeV/c. For this reason even better performances to separate kaons from pions will be obtained. Easy calculation [37] bring to ~ 7.8 sigma the pion – kaon separation angle. Adding conservatively 1.5 sigma, we would obtain a separation ~ 9.3 sigma. This would correspond, assuming a factor ~ 100 for pion-kaon particle population, to a ~ 10^6 power rejection

Convoluting the threshold Cherenkov and the RICH power rejection we would have a pion-kaon power rejection ~ 10^{12}
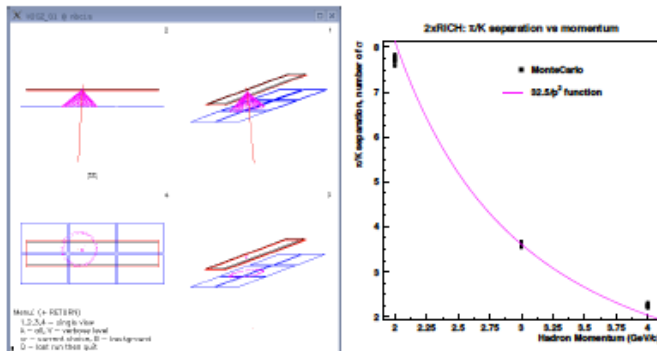
Fig. 9 Upgraded RICH simulation events (left panel) and expected performance (right panel): pion-kaon separation (number of sigmas) at different hadron momenta. The simulation is tuned to the E-94-107 hypernuclear experimental data.
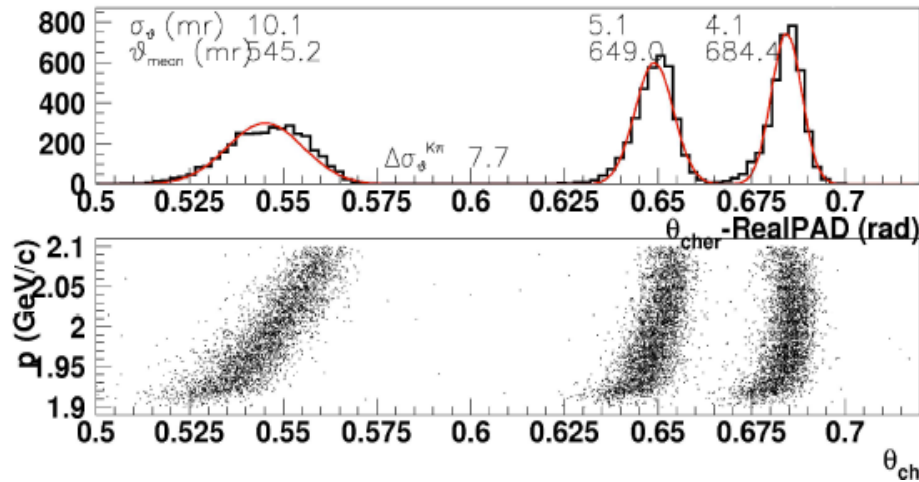
Fig. 10. Upgrated RICH simulated performance. Pion/Kaon angle distribution (equal hadrons populations) at 2 GeV/c momentum, in the HRS acceptance. The Mcarlo is tuned on Hall A hypernuclear experimental data.

5. Kinematics and counting rates

5.1 Kinematics

The definition of the kinematics angles and their limits are illustrated in Fig. 11. This design is based on the kinematics using a 4.5238 GeV beam, minimum HRS angle when using a Septum for an e'momentum at ~3 GeV/c, and maximization of overlap of the virtual photon angular range and the HKS angular coverage to promote the highest possible production yield, while having a sufficiently large separation to completely avoid the forward scattered electrons and positrons.
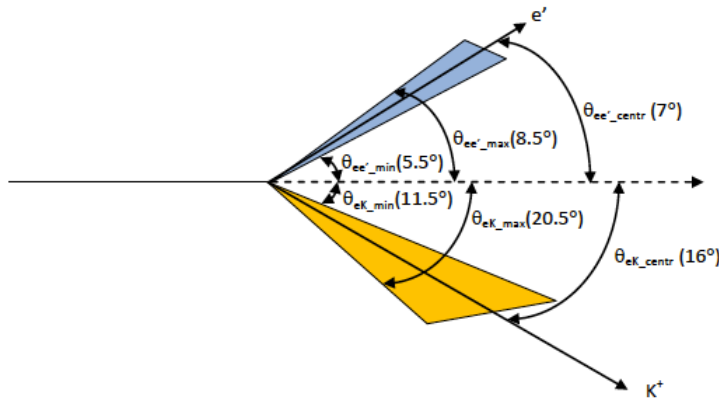
Fig. 11. Kinematics

The kinematics parameters and ranges are listed in Table 2 A GEANT simulation taking into account the realistic and known conditions of HRS and HKS was performed. No acceptance limitation was included for the new Septum magnets which do not yet have detailed engineering design. Details can be found in Paragraph 2.

Table 2. Basic kinematics parameters of the Septum+HRS and Septum+HKS system

Beam energy (12 GeV mode, 2-passes, injector energy included	4.5238 GeV
E' (HRS) central angle (horizontal and vertical bites)	7° (±1.5° and ±2.5

E' (HRS) central momentum (percentage bite)	3.0296 GeV/c (±4.5
Virtual photon central angle ($\phi=\pi$)	13.68°
Virtual photon energy range	1.35 – 1.62 GeV
Virtual photon momentum range	1.40 – 1.70 GeV/
Average Q^2	-0.218 (GeV/c)^2
K^+ (HKS) central angle (horizontal and vertical bites)	16° (±4.5° and ±2.
K^+ (HKS) central momentum (percentage bite)	1.2 GeV/c (±12.5
Lab $\theta_{\gamma K}$ coverage range	0° - 9°

5.2 Counting rates

Using the Millener - Motoba calculations and extrapolating from precedent experiment on ^{12}C the electron, pion and kaon single rates and hypernuclei, as well as the beam time needed for the experiment were evaluated. The cross-section is ~ six times lower than the same reaction on ^{12}C target. The rate of K^+ and the rate of background hadrons in HKS as function of Z and A are known and measured. We estimated the coincidence counting rate for signal and background, assuming a rate of electrons in HRS to be comparable to the value measured in the E94-107 experiment for the same weighted thickness and beam current. This is confirmed by calculation and test measurement performed in Hall A for Apex experiment [Ref. Bogdan Wojtsekhowski, personal communication]. In Table 3 we show the single and coincidences rates for ^{208}Pb as function of the target thickness and beam current. The Signal to Noise ratio is also evaluated for the first 4 peaks (s shell and p shell). We show the Signal to Noise Ratio (Peak significance) defined as S/(sqrt(S+B), where S is the signal (integrated number of counts above the background in the peak) and B the background number of counts below the peak. It should be noted that, due to the large background,s the Signal to Noise ratio doesn't improve too much increasing the target thickness. For this reasons we plan to use a current as high as 25 µA and a target thickness of 100 mg/cm^2. This target thickness in principle allows to obtain an energy resolution ~ 650 keV. However, conservatively, we will assume an Energy resolution of ~ 800 keV.

Tab. 3

Thickness (mg/cm²)	<I> (µA)	(e,e') kHz	(e,k') kHz	(e, π') kHz	Accid.(cps) (e,e')(e,k')Δt	Backgnd (c/h/MEV)	Coinc.(cph) Z(e,e'K+)Z-1 (counts per hour)	Signal to Noise Ratio	Peak
100	25	37	0.07	16	0.01	0.10	0.06	4.3	Shell s (g.s.)
200	25	75	0.14	32	0.04	0.38	0.12	4.7	""
300	25	113	0.21	47	0.10	0.86	0.19	4.9	""
100	25	37	0.07	16	0.01	0.10	0.21	10.5	p
200	25	75	0.14	32	0.04	0.38	0.41	12.8	""
300	25	113	0.21	47	0.10	0.86	0.62	14.0	""

Actually we cannot resolve the g.s. so we will have to sum up the first two levels. The same for the p shell peaks and so on.

The calculations in Tab3 assume a beam time request of 840 hours (5 weeks). The calculation of the background has been extrapolated to the measured values of the precedent experiment on a ^{12}C target.

6. Summary and conclusions

The proposed experiment on ^{208}Pb is an essential part of the campaign of measurements the Jefferson Lab hypernuclear collaboration is proposing to this PAC. It allows to extend the A range of the mass spectroscopy to its extreme. In heavy Λ-hypernuclei, a bound hyperon could be well inside the nucleus free from surface effects. Investigation of deeply bound hypernuclear states in heavy hypernuclei has significance in investigating if a hyperon keeps its identity and is distinguishable as a baryon in a nucleus. The mass dependence of the binding energy for each shell model orbital will be extended to A = 208. It will testify to the validity of a potential to describe hypernuclear states. Moreover, together with the spectroscopy study already performed at Jlab, and proposed to this PAC (namely medium mass spectroscopic study) it will give inputs to the relativistic mean field theories for the calculations of A dependence of Λ single particle energy. The depth of the potential felt by a Λ hyperon can be better determined from the single-particle levels of heavy Λ-hypernuclei, since only a few Λ orbitals are bound in light hypernuclei and information on the Λ potential is limited. The study of the ^{208}Pb(e,e'k) $^{208}_{\Lambda}$Tl reaction together with the other reactions proposed to this PAC by the same collaboration will "complete" the systematic study of Λ hypernuclear bound states over the wide mass range. It will also deepen our understanding of the nature of the ΛN and ΛNN interactions in nuclear medium. This study will allow one to better constrain the current models of the Λ-Nucleon potential, which are at the basis of microscopic calculations of the equation of state of high density hadronic matter. Comparison of standard mean field calculation with ab intio microscopic calculation that include explicitly three body ΛNN interaction will allow to obtain crucial information about their role. This is important also to understand the structure of neutron stars. The good energy resolution will allow to provide important, complementary information with respect to what has been done in the past (and will be done at J-PARC) with hadron probes.

References

1.   D. Lonardoni, S. Gandolfi and F. Pederiva, " Role of the two- and three-body hyperon-nucleon intraction in Λ-hypernuclei, arcXiv:1301.7472v1 [nucl-th] 30 Jan 2013

2.   C.B. Dover, Proc. Int. Sympo. on Medium Energy Physics, Beijing. World Scientifics, Singapore, 1987, p. 257

3.   "Spectroscopy of Λ hypernuclei," Review paper, O. Hashimoto and H. Tamura, Progress in Particle and Nuclear Physics 57 (2006).

4.   T. Hasegawa et al, Phys. rev C53 (1996) 1210

5.   E. Quint, Ph.D. "Limitationd of the Mean – Field Description for nueli in the Pb-region, obeserved with the (e,e'p) Reaction". Thesis Universiteit van Amsterdam 1988.

6.   M.F.Van Batenburg, "Deeply bound protons in ^{208}Pb", Thesis Universiteit van Amsterdam 2001.

7.   F. Garibaldi, S. Frullani, P. Markowitz and J. LeRose, spokespersons, JLab proposal for E94-107.

8.   F. Cusanno et al, Phys. Rev. let. 103, 202501 (2009).

9.   M. Iodice et al. Phys. Rev. Lett. 99, 052501 (2007);

10.   Chapter 13, "New Insights into the Structure of Matter: The First Decade of Science at Jefferson Lab," Editors: D. Higinbotham, W. Melnitchouk and A. Thomas, Journal of Physics: Conference Series, Vol. 299, 2011.

11.   "Shell-model calculations for p-shell hypernuclei," D.J. Millener, Nucl. Phys. A881 (2012) 298.

12.   O. Hashimoto, S.N. Nakamura, L. Tang and J. Reinhold, JLab proposal for E01-011.

13.   O.Hashimoto et al., Nuclear Physics A835 (2010) 121.
14.   F. Garibaldi, S. Frullani, P. Markowitz and J. LeRose, spokespersons, JLab proposal for E94-107.
15.   O. Hashimoto, S.N. Nakamura, L. Tang and J. Reinhold, JLab proposal for E05-115.
16.   F. Cusanno et al, Phys. Rev. let. 103, 202501 (2009).
17.   M. Iodice et al. Phys. Rev. Lett. 99, 052501 (2007);
18.   T. Miyoshi et al., Phys. Rev. Lett. Vol.90, No.23, 232502 (2003); and L. Yuan et al., Phys. Rev. C, Vol. 73, 044607 (2006).
19.   F. Garibaldi, M. Iodice, J. LeRose, P. Markowitz spokespersons, JLab proposal for E07-012.
20.   T. Motoba et al., Strangeness in nuclear and hadronic systems SENDAI08, World Scientific Publishing, ISBN981-4277-60-6 (2010) 178.
21.   B. Sharma, Q.N. Usmani and A.R. Bodmer, arXiv:1102.1542
22.   I. Bobeldij et al. "High-Momentum Protons in 208Pb" Phys. Rev. 73, NUMBER 20 (1994) pg. 2684-2687
23.   O. Benhar, personal communication…
24.   H.-J. Schulze, A. Polls, A. Ramos, and I. Vidana, 73, 058801 (2006)
25.   P.M.M. Maessen, Th.A. Rijken, and J.J. de Swart, Phys. Rev. C 40, 2226 (1989).
26.   Th.A. Rijken, V.J.G. Stoks, and Y. Yamamoto, Phys. Rev. C 59, 21 (1999).
27.   M. Iodice et al., Nucl. Instr. ans Methods A 553, 231 (2005)
28.   F.Garibaldi et al., Nucl. Instr. and Methods A 502, 117 (2003)
29.   F. Cusanno et al., Nucl. Instr. And Methods A 502, 251 (2003)
30.   E. Cisbani et al,. Nucl. Instr. and Methods A 595 (2008) 44–46
31.   R. Michaels, personal communication
32.   W. A Kaufman et al. N ucl. Instr. and Meth. A 335 17 (1993)
33.   J. Alcorn et al. Nucl. Instr. and Methods A 522, 294 (2004)
34.   CERN/LHCC 98-19, ALICE TDR 1, 14 August 1998
35.   Y.Yamamoto, H.Bando, J.Zofka, Progr. Theoret. Phys 80 (1988)757
36.   D.E. Lansky, Y.Yamamoto, Phys. Rev. C55 (1997) 2330
37.   B. Holzenkamp et al., Nucl. Phys. A500, 458 (1989); K. Holinde, Nucl. Phys. A547, 245c (1992).
38.   Y. Yamamoto et al., Prog. Theor. Phys. Suppl. 118, 361 (1994).
39.   R. H. Dalitz and A. Gal, Ann. Phys. 116, 167 (1978).
40.   R. H. Dalitz and A. Gal, Ann. Phys. 116, 167 (1978)
41.   D. J. Millener, A. Gal, C. B. Dover and R. H. Dalitz, Phys. Rev. C 31, 499 (1985).
42.   A. Nogga, H. Kamada and W. Gloeckle, Phys. Rev. Lett. 88 (2002) 172501

6. Summary and conclusion of Part 2

Based on the experience from the hypernuclear physics experiments in both Halls A and C during the 6 GeV era, the new experiments have a chance for further optimization that ensures outstanding and new rich outcomes which may provide key information in the study of hypernuclei and ΛN interactions. This information cannot be obtained nor have such precision by any experiment at any other facility. Therefore, these future experiments are quite unique and important. Furthermore, it is quite cost effective to have the two experiments running together sharing the same beam time with no conflicts. The amount of information to be obtained from the single beam time will be more than the combined outcomes from all previous hypernuclear experiments in both Hall A and Hall C.

Since the two presented options have basically the same quality and yield rate, the remaining decisions depend more on the optimization of the beam schedule, the availability of the utilities in the two halls, *i.e.* ensuring a smooth and maximized physics production once the future beam in 12GeV era becomes available.

Part 3. Decay Pion Spectroscopy of Hypernuclei

Decay Pion Spectroscopy on Light Λ-Hypernuclei

1. Introduction

This part of proposal has been presented twice in the past to PAC33 (C-08-012) [1] and 35 (PR10-001) [2] as well as re-stated as a part of overall program in LOI to PAC39 (LOI-12-003) [3]. This proposal is indeed proposing the experiment to be executed together with the mass spectroscopy part of the proposed experiment using the common overall experimental setup within the same required PAC days of beam time.

Hypernuclei not only bring a strangeness to nuclear physics, they provide a convenient laboratory for obtaining information about the hyperon-nucleon (YN) interaction and explore the full SU(3) symmetry breaking baryon-baryon interaction strong and weak. The existing data on ΛN and ΣN strong interaction are extremely sparse and imprecise: production and scattering in the same target are required due to low hyperon beam intensities and short lifetimes. There are several realistic models for the free YN interactions, based on boson exchanges. Well-known are YN potentials of the Jülich group [4] constructed along the same guidelines as used in the Bonn NN potential. The Nijmegen group [5] for many years has developed several one-boson exchange potential models. They use SU(3) constrains on the coupling constants to fit about 4300 pp+np data on cross sections and variety of spin correlation together with 35 scattering ΛN and ΣN data at low energies. Since the empirical information on YN scattering consists almost exclusively on spin-averaged quantities like total and differential cross sections, the spin structure of the free YN interaction is essentially unknown. Therefore, various models for the YN interaction, which differ widely in their spin (and isospin) dependence, are able to describe the same scattering data. The only way to obtain low-momentum data is from hypernuclear spectroscopy: the results of hypernuclear structure calculations are sensitive to the spin dependence of the YN interaction and the finite-nuclei YN G-matrix provide a useful tool for testing the spin structure of the various YN interactions. Several authors [6, 7] have analyzed the ΛN effective interaction for p-shell nuclei in terms of five phenomenological parameters V, Δ, S_Λ, S_N and T. High precision data on light hypernuclei are of vital importance for the accurate determination of the missing parts of the YN interaction. Currently, there exist not only reliable methods for identification phenomenological strong interaction ΛN, but also first attempts to relate it to modern Lattice QCD techniques [8].

In the last thirty years a new branch of nuclear physics, namely physics of nuclei in the vicinity of the neutron drip line has been constituted [9]. Hypernuclear Physics could be used in the studies of the loosely bound nuclear systems such as the nuclei with neutron halo. In addition, the role of Λ in the nuclear medium with pure baryonic interactions may be more clearly distinguished.

The lightest unstable–core hypernucleus $^6_\Lambda$H is a good example. It was predicted by Dalitz and Levi Setti [10], and has attracted attention even at "emulsion era" of hypernuclear physics. It was considered possible to be formed in ^{6}Li- ^{7}Li-loaded emulsion: $K^- + {}^6$Li (^{7}Li) $\rightarrow \pi^+ + {}^6_\Lambda$H + $p(d)$. The three body decay mode, $^6_\Lambda$H $\rightarrow \pi^- + t + t$, was searched for in [11] but no decay at all was found. Very recently, FINUDA Collaboration considered both the production and decay in coincidence:

$$K^-_{stop} + {}^6\text{Li} \rightarrow {}^6_\Lambda\text{H} + \pi^+ \; (\sim 250 < p_{\pi+} < 255 \text{ MeV/c})$$

$$^6_\Lambda H \rightarrow \, ^6He + \pi^- \; (\sim 130 < p_{\pi^-} < 137 \; \text{MeV/c})$$

and found three events corresponding to the formation and subsequent decay of $^6_\Lambda H$ [12] with the result in $B_\Lambda(^6_\Lambda H) = 4.0 \pm 1.1$ MeV. This value appears to agree well with a theoretical estimation [13].

The interest and efforts of study hypernuclei and anti-hypernuclei continues around world (Japan, Europe, and USA) with various production mechanisms using the beams of mesons ($K^\pm$ and $\pi^\pm$), electrons, and relativistic heavy ions. One of the irreplaceable uniqueness of the JLab experiments using the CEBAF beam and electroproduction mechanism is the precision in determining B_Λ. Other features are discussed in detail in the mass spectroscopy part of proposal. The high precision γ spectroscopy program [14] using the (π^+, $K^+\gamma$) and (K^-, $\pi^-\gamma$) reactions has been very successful in measuring precisely the level spacing for a sequence of p-shell hypernuclei. However, no ground state B_Λ could be determined.

In parallel to the proposed experiments to study the elementary production process of Λ hyperon and to investigate the detailed hypernuclear level structure in wide mass range with high precision, this part of experiment to be run parasitically intends to use high precision monochromatic π^-'s from the unique two-body mesonic weak decay of hypernuclei to investigate ground state of light Λ-hypernuclei with variety of (Z, A) combinations through hyperfragments from largely produced hypernuclear continuum in the ($e,e'K^+$) electro-production. A collection of hypernuclei: neutron-rich hypernuclei, neutron drip line hypernuclei (including $^6_\Lambda H$ and $^8_\Lambda H$) and mirror pairs of hypernuclei can be observed. The binding energy of their ground states can be measured with the highest possible precision.

The principle of this experiment can be illustrated by the following production and decay processes:

Step 1: $e + \, ^AZ \rightarrow e' + K^+ + [^A_\Lambda(Z\text{-}1)^*$, hypernuclei at higher excitation]

Step 2: $^A_\Lambda(Z\text{-}1)^* \rightarrow$ [variety of hyperfragments] + [nuclear fragtments]

Step 3: Hyperfragment$_{stop} \rightarrow$ [converted non-strange nucleus] + π^-_{mono}.

Step 1 is the production of the primary hypernuclei at higher excitation (continuum). The primary hypernuclei fragment when the masses are above the nuclear break up threshold and variety of light hypernuclei with various (Z, A) combination is produced. They stop in target quickly. Step 3 is only the two body mesonic weak decay channel from which the monochromatic π^- will be detected and analyzed for its momentum. The momentum of π^- directly reflects the B_Λ of the decayed hyperfragment at its ground state. It may also show the low lying excitation of the converted non-strange nucleus. Such excitation features directly the ground state spin-parity of the decayed hyperfragment due to angular momentum selectivity. It is much easier to reach the highest possible precision by analyzing the momentum of a single monochromatic particle using a high quality spectrometer. The yield rate is mainly affected by the acceptance at each step of the entire production and decay processes.

The high precision result will have important impact to the following three (but not the least) major areas:

1. Precise B_Λ and determination of spin-parity of the ground state of variety of light hypernuclei will provide stringent limit for the YN interaction model. In combination with the high precision level structure measurements and γ spectroscopy, the phenomenological parameters V, Δ, S_Λ, S_N and T in the ΛN effective interaction can be better determined. Results from the early emulsion experiments are still playing important role in determining these parameters [15, 16] in combination with the most recent high precision γ-spectroscopy observations [14]. Results from this experiment may improve some of the emulsion results which had poor statistics.

2. Precise B_Λ from iso-spin mirror pair hypernuclei will be used to study the charge symmetry breaking in the ΛN interaction. The puzzle resulted from the $^4_\Lambda$H and $^4_\Lambda$He pair (i.e. inconsistency in the separations of their ground states and their 1st excitation states) is unresolved. The experiment aims to be able to identify couple of mirror (iso-spin doublets) pairs in one measurement within the variety of (Z, A) combinations so that the separation can be directly measured. In addition, precision results from some neutron rich light hypernuclei can provide information for such investigation when paired with results to be measured by other means such as future experiments at J-PARC.

3. The neutron rich and neutron drip line light hypernuclei provide valuable information on the iso-spin dependence and Λ-Σ coupling in the ΛN interaction in nuclear medium. The Λ-Σ coupling effect is much more clearly exposed in case of light neutron rich hypernuclei. Confirmation and precise B_Λ measurement of $^6_\Lambda$H is significant for both the hypernuclear and non-strangeness nuclear physics. Another neutron excess light hypernucleus is possible existence of $^8_\Lambda$H in which the glue-like role of Λ to unstable nuclear core extends to its extreme. It will be exciting if it can be proven exist. There are many other interesting light hypernuclei with neutron excess may exist, for example $^9_\Lambda$He.

4. The yield ratio measured in one experiment between the observed light hypernuclei may help to understand the fragmentation mechanism, selectivity in forming hyperfragments, and the composition of the continuum.

2. MAMI test runs

Inspired by the opportunity offered by the monochromatic decay π^-, a pioneering feasibility test experiment [17] was carried out twice (each with only short beam time) at MAMI-C by the hypernuclear physics part of the A-1 collaboration in 2011 and 2012.

The KAOS spectrometer was used at zero degrees to tag the K^+'s associated with Λ and Σ production. The scattered electrons passed through KAOS without detection. The spectrometer Spec-C was used at a backward angle as the proposed JLab experiment to detect the decay π^-'s. The Be target foil is tilted with respect to the beam but facing normal to Spec-C to increase the primary hypernuclear production while to minimize the target straggling by the decay π^-'s. Spec-C is a well-known spectrometer and the π^-'s were well identified. However both runs encountered severe problems from background in the K^+ identification.

For the 2011 run, the positrons from pair production at near zero degrees overwhelmed the singles rate in the K^+ arm, causing extremely high online coincidence trigger rate due to positron accidentals. Thus, the beam current was forced to be reduced to only 1μA. In offline analysis,

the kaon identification detector system and the time-of-flight (TOF) were ineffective in separating K^+'s from π^+'s and e^+'s. Therefore, the coincident π^- momentum spectrum had high accidental backgrounds from all mis-identified particles (see Fig. 1 top).
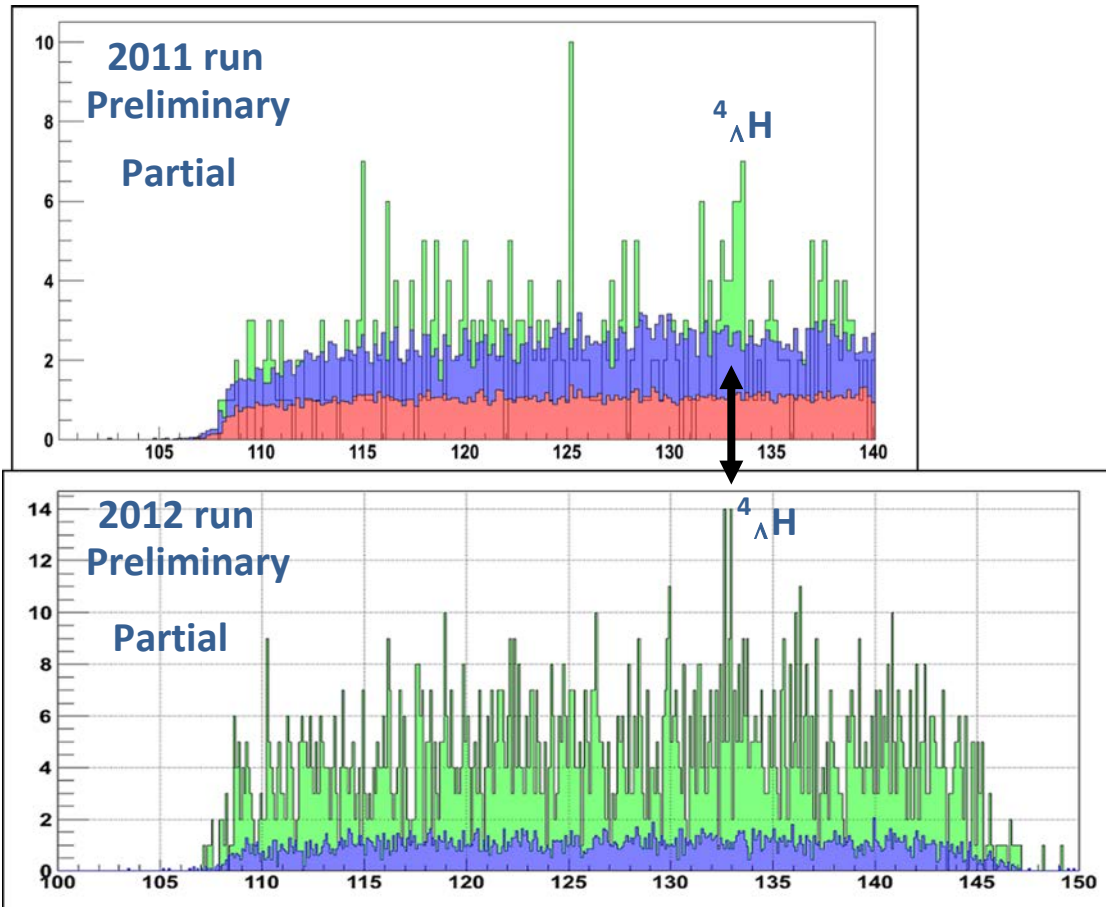

Figure 1. Comparison of the π^- momentum spectra obtained by the 2011 and 2012 runs. Observation of the $^4_\Lambda H$ hypernuclei is evidential, although both runs had low yield rate due to limitation from the kaon arm and high accidentals from background particles.

For the 2012 run, a 10cm thick lead curtain was inserted before other detectors. It removed almost all positrons so that the beam current was able to be increased to 20μA. However, a GEANT4 simulation showed that the K^+ survival rate from this lead degrader is only about 30%. In addition, this degrader caused a further decrease of survival rate from the lifetime of K^+'s and a further decrease of the detection efficiency. Therefore, the overall increase of the yield rate is only about 3.5 times over the 2011 run condition even the beam current was increased by 20 times. There were additional problems for the detectors, such as the KAOS fringing magnetic field in the axial direction of the 5" PMT tubes used for the aerogel Čereknov detector. Thus separation of K^+'s from background particles was still challenging (see Fig. 1 bottom).
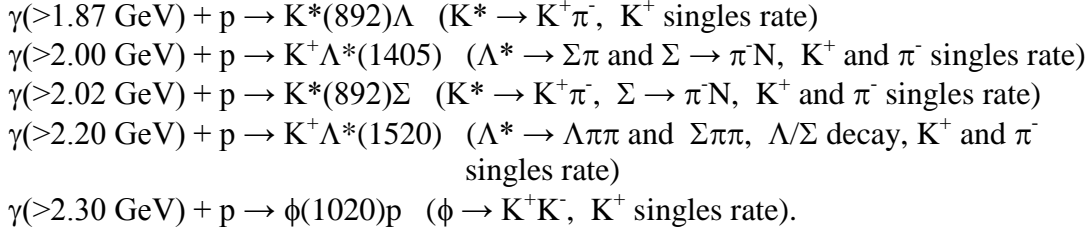
Although the collaboration is considering the future run plan (possibly in 2014), the problems from the KAOS remain quite challenging to be fully resolved or optimized. Nevertheless, the preliminary spectra (Fig. 1) in comparison between the two runs provided encouraging evidence

of observing the $^4_\Lambda$H hypernucleus that was expected to have the highest production yield among all the light hypernuclei according to the statistical model on the nuclear fragmentations from one nucleus.

3. Basic technique of the proposed JLab experiment

The basic principle for the JLab experiment in terms of study the momentum spectroscopy of the two-body mesonic decay π^-'s from light hyperfragments is identical as that for the MAMI-C experiment. The main differences are in (1) kinematics and (2) the experimental configuration and technique.

For the JLab experiment, 4.52 GeV beam will be used while the MAMI-C used 1.508 GeV beam. The JLab experiment tags K$^+$'s by the HKS spectrometer at a lab angle of 16° with a solid angle acceptance of 10 msr and a momentum range from 1.05 GeV/c to 1.35 GeV/c. This corresponds to a photon energy range from 1.35 to 1.62 GeV for the Λ production. KAOS detects K$^+$'s at 0° with a solid angle acceptance of 25 msr and a momentum range from 0.675 to 1.125 GeV/c so that the corresponding photon energy is from 1.02 to 1.41 GeV. The average 3-momentum transfer that affects the form factor of the hypernuclei is different for the two experiments. For the JLab experiment it is 480 MeV/c while it is 370 MeV/c for the MAMI-C experiment. The kinematics difference makes differences (but not significantly) for the sources of background and the physics production yield rate. For example, the actual photon energy range is sufficiently large for the JLab so that additional K$^+$ production channels are open. These are:

$\gamma(>1.87 \text{ GeV}) + \text{p} \rightarrow \text{K*}(892)\Lambda$ (K* $\rightarrow$ K$^+\pi^-$, K$^+$ singles rate)

$\gamma(>2.00 \text{ GeV}) + \text{p} \rightarrow \text{K}^+\Lambda\text{*}(1405)$ ($\Lambda^* \rightarrow \Sigma\pi$ and $\Sigma \rightarrow \pi^-\text{N}$, K$^+$ and π^- singles rate)

$\gamma(>2.02 \text{ GeV}) + \text{p} \rightarrow \text{K*}(892)\Sigma$ (K* $\rightarrow$ K$^+\pi^-$, $\Sigma \rightarrow \pi^-$N, K$^+$ and π^- singles rate)

$\gamma(>2.20 \text{ GeV}) + \text{p} \rightarrow \text{K}^+\Lambda\text{*}(1520)$ ($\Lambda^* \rightarrow \Lambda\pi\pi$ and $\Sigma\pi\pi$, Λ/Σ decay, K$^+$ and π^-
singles rate)

$\gamma(>2.30 \text{ GeV}) + \text{p} \rightarrow \phi(1020)\text{p}$ ($\phi \rightarrow$ K$^+$K$^-$, K$^+$ singles rate).

Background and physics yield rate will be discussed in more detail in later sections.

As shown in Appendix I, the post beam and near zero degree scattering particles will not enter any spectrometer for the JLab experiment. This dramatically reduces the challenge in the K$^+$ detection. The HKS has well established K$^+$ identification system which has demonstrated capable to separate the K$^+$'s from backgrounds cleanly in the last two experiments, E01-011 and E05-115. The detector system contains 3 layers of TOF counters, 3 layers of aerogel Čerenkov detectors, and 2 layers of water Čerenkov detectors, all optimized for kaon identification at the designed momentum range. More than 98% of background particles were removed at the online level so that the accidental coincidence trigger rate for the decay π spectroscopy experiment will be kept at minimum as about less than 10Hz with maximized beam current, i.e. up to 100μA. The estimated maximum online singles rates with minimum particle identification for K+ and π- are 10kHz and 20kHz, respectively. The online time coincidence window is 40ns. Targets for both the mass spectroscopy and decay π spectroscopy experiments are taken into account.

Although for illustration purpose, the experimental configuration layout shown in Fig. 1 in Appendix I showed only the HES spectrometer as the decay π spectrometer, in actual experiment

the Enge spectrometer will also be mounted about 180 degrees with respect to the HES spectrometer. In other words, there will be two spectrometers to detect the decay π^-s, doubling the physics yield. Similarly, the MAMI-C experiment used both Spec-C and Spec-A spectrometers although only partial analysis from Spec-C was shown in Fig. 1. The momentum acceptance of both these two spectrometers is large and covers the entire interested momentum range from 88 to 140 MeV/c. In case of the MAMI-C experiment, the momentum acceptance for both Spec-C and –A is smaller than the needed range. Therefore, they were set to complement to each other with an overlap region to check consistency. For the JLab experiment, the two spectrometers can cross calibrate and check each other for consistency in the full physics range and the results can be summed.

The target incline angle with respect to the beam will be smaller for the JLab experiment so that both the spectrometers will be close to the normal direction to the beam. Engle spectrometer has smaller solid angle acceptance and will be mounted slightly forward at 70° to the beam while HES will be at -110° due to its larger solid angle acceptance. This arrangement is an optimization against the background π's (see later discussions).

Both the existing HES and Enge spectrometers have excellent momentum resolution better than 3×10^{-4} FWHM. The central momentum will be at 114 MeV/c with a momentum acceptance from 88 MeV/c to 140MeV/c. The target straggling energy uncertainty is at level of 75keV (see simulation result shown in Ref. 2), dominating the overall resolution. The averaged overall momentum uncertainty is better than 165keV/c FWHM.

Detector system for the π^- spectrometers is conventional type. It includes: (1) track wire chambers for the momentum analysis and the TOF correction and (2) two layers of scintillation counters (one thin layer and one thick layer) separated by 1.0 meter for TOF and time coincidence with K^+'s plus a dE/dx analysis. Both the μ^-'s and π^-'s are in the similar β range, from 0.54 to 0.8. However, in the interested momentum range π^-'s loss about 30% more energy than μ^-'s. The e^-'s are the $\beta = 1$ particles. Therefore, π^-'s can be easily separated by the correlation between β and the total dE/dx.

To avoid confusion here it must be pointed out that the kinematics for the mass spectroscopy experiment by the (e, e'K^+) reaction and the decay π spectroscopy experiment without tagging on e' are different. The momentum and angle of the tagged e' make the virtual photons aiming to the HKS setting angle, i.e. $\theta_{\gamma K} = 0°$ with energy averaged at 1.5 GeV. Therefore the 3-momentum transfer is ~300 MeV/c. The production cross section reduction comes from Q^2 increase from ~0 to -0.2 $(GeV/c)^2$. In case of the decay π spectroscopy experiment, photons at near zero degrees are primarily considered so that $\theta_{\gamma K} = 16°$. This makes the 3-momentum transfer larger. In other words, although the two experiment sharing the same K^+ singles from HKS, actually each access different portion of it for physics except accidentals. Of course, they will also be separated physically from their own targets.

4. Yield estimation comparison to the MAMI-C results

The overall yield is affected by two parts: (1) the production kinematics of the primary hypernuclei at high excitation (in the continuum) and (2) the experimental configuration, when comparing to the MAMI-C experiment.

4.1 Kinematics

Both the MAMI-C and the proposed JLab experiments tag K^+ only without detecting the scattered e'. The K^+ momentum range defines the corresponding scattering angle and momentum ranges of untagged e's.

As mentioned the proposed JLab experiment will use 4.52 GeV electron beam while the MAMI-C beam was at 1.508 GeV. The total integral of virtual photon flux factor, $\int \Gamma d\Omega dE'$, with the corresponding $\Delta E'$ for the JLab experiment is **1.8** times higher than that of the MAMI-C experiment.

The 3-momentum transfer for the Jlab experiment is higher (~480 MeV/c) than that of the MAMI-C experiment (~370 MeV/c). Such increase reduces cross section for the ground and low lying states of the primary hypernuclei. However, they are not the sources for the hyperfragments. The light hypernuclei formed by fragmentation actually come from highly excited states of hypernuclei in the continuum region. The higher 3-momentum transfer actually enhances the yield of the high excitation states. Until now, the exact formation of the continuum is not well understood. However, using the theoretically predicted high excitation states (cross sections and excitation energies) folded with assumed 3MeV FWHM width appears agreed well for the quasi-free production distribution for at least the excitation energy region 30 MeV above the Λ production threshold. The production ratio of the continuum in the region of the first 30 MeV above threshold over the total production in the bound region for the case of $^{12}_{\Lambda}C$ [14] can be used to make estimation and singles out only the q dependence. The ratio in the spectrum from the $^{12}C(K^-, \pi^-)^{12}_{\Lambda}C$ is ~1:1 with q ~ 100 MeV/c, while that from the $^{12}C(\pi^+, K^+)^{12}_{\Lambda}C$ is ~1:3 with q ~ 300 MeV/c. Many more additional excited states from Λ at higher orbits or s-shell hole nuclear core states can be produced with higher momentum transfer. In other words, the total cross section for high excitation states in the continuum region may actually increase as q increases. Thus, using this ratio to make production yield estimate, the JLab experiment may have about a factor of **1.29** higher physics yield rate than that from the MAMI-C experiment.

Therefore, the overall gain factor from the kinematics differences is ~**2.32** times.

4.2 Experimental configuration

In case of the experimental technique differences, an itemized comparison between the JLab and the 2012 MAMI-C experiment (second run) in terms of yield gain factors is shown in Table 1. This is the experimental part of the differences. The two spectrometers, HES and Enge, are independent, and each acts like a single experiment. If the spectra obtained by HES and Enge can be summed, the total experimental technique gain factor will be **3.83**.

Table 1. Itemized configuration gain factors in comparison to the MAMI-C experiment. The K^+ detection by HKS is common for both HES and Enge so that the gain factors related to K^+ are the same.

	MAMI-C	JLab/ HES	Gain Factor	JLab/ Enge	Gain Factor
Applicable beam current (µA)	20	80	4.0	80	4.0
Target thickness (mg/cm^2)	22.56	22.56	-	22.56	-

Target incline angle (degrees)	54	65	-	65	-
Effective target thickness (mg/cm^2)	38.38	53.38	1.39	53.38	1.39
Kaon arm solid angle (msr)	25	9	0.36	9	0.36
Kaon survival rate (lifetime and Pb blocking)	0.12	0.29	2.42	0.29	2.42
Kaon detection efficiency	0.8	0.8	1.0	0.8	1.0
Pion arm solid angle (mrs)	28	8	0.29	6	0.21
Pion survival rate	0.33	0.459	1.39	0.604	1.83
Overall gain factor			**1.93**		**1.9**

Combining gain factors from both the production kinematics and the experimental technique, the overall gain over the MAMI-C experiment is about **8.89**.

4.3 Estimated yield

The total running time calculated based on the integrated charge on target is 222 hours and the total scaled yield of $^4_\Lambda$H is about 30 counts. This gives a yield rate of ~0.14 counts/hour for the MAMI-C experiment. Applying the overall gain factor of 8.89 for the proposed JLab experiment, a 1.24 counts/hour yield rate for the $^4_\Lambda$H observation is expected by the proposed JLab experiment.

5. Backgrounds

The second run of the MAMI-C experiment using 20µA beam showed a Spec-C singles rate about 30kHz. If applying a simple scale up from Table 1, HES and Enge will have about 85kHz singles rate. However, the kinematics difference makes the singles rate different. Since the JLab experiment uses much higher beam energy (4.52 GeV), the phase space is folded much more forward. Most of the π^-'s from two body reactions are at forward direction, avoiding the HES and Enge spectrometers. Thus, this part of the π^-'s singles is actually dramatically reduced except those from three-body reactions or from the multiple decay processes from the newly opened channels described in Section 3. Therefore, it is anticipated that the π^- singles rate remains around 20kHz for each of the HES and Enge spectrometer.

Due to these newly opened channels, the K^+ singles rate is expected to increase up to 2kHz. Thus the accidental K^+ and π^- coincidence background yield rate is about 3 times higher than that from the MAMI-C experiment with lower beam current. The total background in the MAMI-C spectrum is actually dominated by the mis-identified K^+'s. The true accidental background from the K^+ and π^- coincidence is only about 20% of the overall background height. Thus the accidental background yield is about 60% of the total from the MAMI-C experiment.

The primary real K^+ and π^- coincidence background for the MAMI-C experiment is from the Σ production with $\Sigma^- \rightarrow \pi^-$n and $\Sigma^\circ \rightarrow \gamma\Lambda$ followed by $\Lambda \rightarrow \pi^-$ p and. In case of the JLab experiment, due to higher momentum transfer, this background will be reduced significantly. However, the newly opened K^+ channels supplement such reduction, adding additional real K^+ and π^- coincidence background. The rate from these channels depends on their production cross sections with K^+ detected at large $\theta_{\gamma K}$ angle (16°). Although there will be no background from mis-identified K^+'s, these open channels raises the background yield up. Overall, the similar

background yield rate is expected and it is about **0.027counts/hour/bin**, if the same bin size is used for the π^- momentum spectrum.

6. Target, required beam time and goal of statistics

The proposed JLab experiment will use either a 22.56 mg/cm^2 ^{9}Be or ^{12}C target, depending on the future MAMI-C plan on this program. If the MAMI-C collaboration continues to focus on using the ^{9}Be target in the next a few years to build statistics and see no complication in terms of detailed spectroscopy, the ^{12}C target may become the primary goal since it gives chance to search for the heaviest hydrogen-like hypernucleus $^8_\Lambda$H.

The production yield rate for the $^4_\Lambda$H hypernuclei extracted from the MAMI-C spectrum is about 0.14counts/hour. Thus the corresponding rate for the JLab experiment will be 1.24counts/hour. This experiment proposes a total of 70 days of data collection time. The total number of counts for the $^4_\Lambda$H hypernuclei will be about 2090 counts combined from HES and Enge. The background height will be about 45 counts/bin. Although hyperfragment has been a very interesting topic but there has not been an effective experimental effort to give information about the yield rate. A statistical model is commonly used for nuclear fragmentation in heavy nuclear mass region. There is no verification that it works well in the light mass region. Nevertheless, estimate based on this model shows that the yield rate is decreasing fast as the fragment mass increases. The yield rate for the heaviest fragment can be more than 20 times smaller than the lightest one, $^4_\Lambda$H. The spin-iso-spin selectivity may enhance the yield for certain hyperfragments. Thus the experiment may for the first time to provide important experimental evidence for the yield ratio of variety of hyperfragments from one primary hypernuclear production and to lead better understanding on the formation of the continuum. Therefore, the required total beam time is aiming to observe the hyperfragment which may have yield as small as only about 100 counts in total with a signal over background ratio of about 1:1.

7. Summary

Decay π^- spectroscopy can open a new frontier in hypernuclear physics, obtaining precise B_Λ for the ground state of variety of light hypernuclei through fragmentgation of highly excited states of the primarily produced hypernuclei. It allows searching for the heaviest neutron rich hypernuclei in the light mass region. Although the MAMI-C experiment experienced severe challenge on the K$^+$ identification due to the extreme kinematics condition at zero degrees, it does confirm the $^4_\Lambda$H production from fragmentation and provides important parameters with which we can make reasonably reliable estimates on the physics yield and background. The proposed experiment will share the same beam with the separately proposed mass spectroscopy experiments but different targets. The requested beam time is based on observation of the hypernuclei which have yield rate up to 20 times smaller than that of $^4_\Lambda$H. Some of them are extremely interesting, such as $^6_\Lambda$H and $^8_\Lambda$H.

References

1. L. Tang at el., "Study of Light Hypernuclei by Pionic Decay at JLab", proposal C-08-012 (rating A-), JLab PAC33, 2008.
2. L. Tang at el., "Study of Light Hypernuclei by Pionic Decay at JLab", proposal PR10-001, JLab PAC35, 2010.
3. L. Tang at el., "Study with High Precision on Electro-production of Λ and Λ-Hypernuclei in Full Mass Range", LOI 12-003, JLab PAC39, 2012.
4. A.G. Reuber, K. Holinde, J. Speth, Czech. J. Phys. 42, 1115 (1992).
5. Th.A. Rijken, Nucl. Phys. A691, 322c (2001).
6. D.J. Millener *et al.,* Phys. Rev. C31, 449 (1985).
7. V.N. Fetisov *et al.,* Z. Phys. A339, 399 (1991).
8. S.R. Beane *et al.,* arXiv:1206.5219.
9. B. Jonson, Phys. Reports 389, 1 (2004).
10. R.H. Dalitz, R. Levi Seti, N. Cimmento 30, 489 (1963).
11. W. Gajewski *et al.*, Nucl. Phys. B2, 288 (1967).
12. M. Agnello *et al.* (FINUDA Collaboration and A. Gal), Phys. Rev. Lett. 108, 042501 (2012); Nucl. Phys. A881, 269 (2012).
13. L. Majling, Nucl. Phys. A585, 211c (1995).
14. O. Hashimoto, H. Tamura, Progr. Part. Nucl. Phys. 57, 564 (2006).
15. D.J. Millener, Nucl. Phys. A881, 298 (2012).
16. D.H. Davis, J. Pniewski, Contemp. Phys. 27 (1986) 91; D.H. Davis, Nucl. Phys. A 754 (2005) 3c.
17. P. Auerbach *et al.* (A1 Collaboration), Nucl. Phys. A881, 187 (2012).

Part 4. Summary

Based on more than a decade experiences at JLab Hall-A and C, the JLab Hypernuclear Collaboration proposes a comprehensive programs of the hypernuclear study in full mass range:

1. Elementary Λ production,

2. Few-body hypernuclear production,

3. Medium mass hypernuclear production,

4. Heavy hypernuclear production,

5. Decay pion spectroscopy.

Program 1 was an update of 6 GeV approved experiment E07-012, a part of program 3 (Ca target) is update of conditionally approved experiment C08-002, and program 5 is update of the conditionally approved experiment C08-012, C12-10-001.

All experiments share the same beam conditions and major apparatus as follows.

Here, we summarize important parameters and required resources for conducting of the experiment.

Key Experimental Parameters:

Beam energy: 12 GeV mode, 2-pass : 4.5238 GeV, Hall-A,

Requesting beam time in total: 15 weeks = 105 days.

Range of beam currents: 2 to 100 μA,

Major apparatus: HKS, HRS, Speta, HES and ENGE

Required resources:

Major installations and new support structures:

HKS, Septa, HES and ENGE need major installation of magnets and detector packages.

HES has height adjustable support, but HKS needs to build a new support instead of support structure designed for Hall-C.

New support structure for Septa, ENGE, Shielding houses for detectors are necessary.

Major Equipment

Magnets: HRS in Hall A, HKS (KQ1, KQ2 and KD), HES (EQ1, EQ2 and ED), ENGE Split-pole magnet, new Septum magnets (one might be previously used super-conducting septum)

PS: HKS-D, HES-D have own PS provided by Tohoku Univ. ,

all other PS's are necessary to be prepared by JLab.

Targets: Cryo-target for liquid H_2 and ^{4}He.

Solid targets: CH_2, ^{12}C, ^{40}Ca, ^{44}Ca, ^{48}Ca, ^{27}Al, ^{48}Ti, ^{208}Pb.

Detectors: Standard detectors for HRS,

HKS-detector package (Drift Chambers, TOF walls, Aerogel Chrenkov, Water Cherenkov)

HES-dectector package (Drift Chamber, TOF walls)

ENGE detector package (Drift Chamber, TOF walls)

Electronics: Standard electronics, F1-TDCs, Amp-discriminator cards for drift chambers

FPGA based special trigger modules developed by Tohoku Univ.(TUL-8040)

Computer Hardware : Standard

Possible Hazard

Cryogenics: Standard cryotarget in Hall-A

Electrical Equip.: high voltages for PMT, Drift Chambers, large currents for magnets

Flammable gas for drift chambers: Argon Ethane 50/50, 0.15 l/min each for HRS, HKS, HES and ENGE

Targets: 1 & 2 are for calibration, 3-8 are for (e,e'K) hypernuclear spectroscopy and 9 for decay pion spectroscopy of electroproduced hypernuclei.

Condition #	Beam Energy(MeV)	Beam Current (μA)	Special Request	Target Material	Material Thickness (mg/cm^2)	Est. Beam on time (hours)
1	4523.8	2	2×2 mm^2 raster	CH_2	500	120
2	4523.8	100	Unrastered	^{12}C	100	216
3	4523.8	100	3×3 mm^2 raster	Liq. H_2	283	168
4	4523.8	10	1.5×1.5 mm^2 raster	Liq. ^{4}He	500	263
5	4523.8	100	Unrastered	^{40}Ca	100	240
6	4523.8	100	Unrastered	^{44}Ca (^{48}Ca)	100	178
7	4523.8	100	Unrastered	^{48}Ti	100	213
8	4523.8	25	2×2 mm^2 raster	^{208}Pb	100	840
Sub total						**2238**
9	4523.8	Shared with (e,eK)		^{7}Li, ^{9}Be, ^{12}C	53	(1680) Included in the above